

## Identification, optimization and pharmacology of acylurea GHS-R1a inverse agonists

William McCoull, Peter Barton, Alastair Brown, Susanne Bowker, Jennifer Cameron, David Clarke, Robert Davies, Alastair Dossetter, Anne Ertan, Mark Fenwick, Clive Green, Jane Holmes, Nathaniel Martin, David Masters, Jane Moore, Nicholas Newcombe, Claire Newton, Helen Pointon, Graeme R. Robb, Christopher Sheldon, Stephen Stokes, and David Morgan

*J. Med. Chem.*, **Just Accepted Manuscript** • DOI: 10.1021/jm500610n • Publication Date (Web): 26 Jun 2014

Downloaded from <http://pubs.acs.org> on July 6, 2014

### Just Accepted

“Just Accepted” manuscripts have been peer-reviewed and accepted for publication. They are posted online prior to technical editing, formatting for publication and author proofing. The American Chemical Society provides “Just Accepted” as a free service to the research community to expedite the dissemination of scientific material as soon as possible after acceptance. “Just Accepted” manuscripts appear in full in PDF format accompanied by an HTML abstract. “Just Accepted” manuscripts have been fully peer reviewed, but should not be considered the official version of record. They are accessible to all readers and citable by the Digital Object Identifier (DOI®). “Just Accepted” is an optional service offered to authors. Therefore, the “Just Accepted” Web site may not include all articles that will be published in the journal. After a manuscript is technically edited and formatted, it will be removed from the “Just Accepted” Web site and published as an ASAP article. Note that technical editing may introduce minor changes to the manuscript text and/or graphics which could affect content, and all legal disclaimers and ethical guidelines that apply to the journal pertain. ACS cannot be held responsible for errors or consequences arising from the use of information contained in these “Just Accepted” manuscripts.



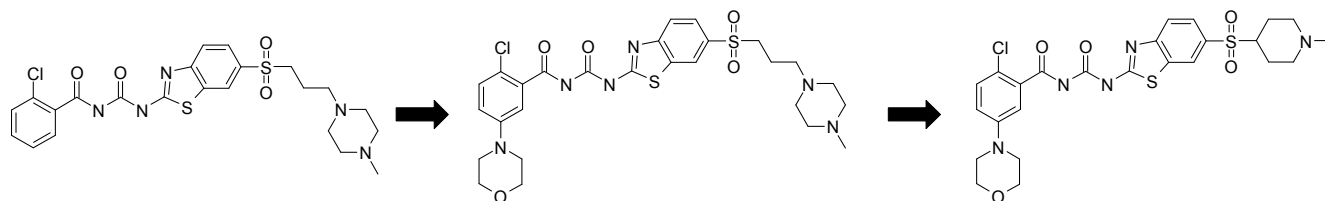
## Identification, optimization and pharmacology of acylurea GHS-R1a inverse agonists

William McCoull,\* Peter Barton, Alastair J.H. Brown, Suzanne S. Bowker, Jennifer Cameron, David S. Clarke, Robert D.M. Davies, Alexander G. Dossetter, Anne Ertan, Mark Fenwick, Clive Green, Jane L. Holmes, Nathaniel Martin, David Masters, Jane E. Moore, Nicholas J. Newcombe, Claire Newton, Helen Pointon, Graeme R. Robb, Christopher Sheldon, Stephen Stokes and David Morgan  
*AstraZeneca, Mereside, Alderley Park, Macclesfield, SK10 4TG, UK*

### KEYWORDS

Ghrelin; Growth hormone secretagogue receptor type 1a; inverse agonist; antagonist; GHS-R1a; CNS penetration; Food intake; Pharmacokinetics; Synthesis.

### ABSTRACT



Compound	<b>14</b> (AZ-GHS-14)	<b>22</b> (AZ-GHS-22)	<b>38</b> (AZ-GHS-38)
GHS-R1a binding IC <sub>50</sub>	1.3 nM	0.77 nM	6.7 nM
GHS-R1a function	partial agonist	inverse agonist	inverse agonist
CNS exposure	-	non-CNS penetrant	CNS penetrant

1 Ghrelin plays a major physiological role in the control of food intake and inverse agonists of the ghrelin  
2 receptor (GHS-R1a) are widely considered to offer utility as anti-obesity agents by lowering the set-  
3 point for hunger between meals. We identified an acylurea series of ghrelin modulators from high  
4 throughput screening and optimized binding affinity through SAR studies. Furthermore, we identified  
5 specific substructural changes which switched partial agonist activity to inverse agonist activity, and  
6 optimized physicochemical and DMPK properties to afford the non-CNS penetrant inverse agonist **22**  
7 (AZ-GHS-22) and the CNS penetrant inverse agonist **38** (AZ-GHS-38). Free feeding efficacy  
8 experiments showed that CNS exposure was necessary to obtain reduced food intake in mice and it was  
9 demonstrated using GHS-R1a null and wild-type mice that this effect operates through a mechanism  
10 involving GHS-R1a.  
11  
12  
13  
14  
15  
16  
17  
18  
19  
20  
21  
22  
23  
24  
25  
26  
27  
28  
29  
30  
31  
32  
33  
34  
35  
36  
37  
38  
39  
40  
41  
42  
43  
44  
45  
46  
47  
48  
49  
50  
51  
52  
53  
54  
55  
56  
57  
58  
59  
60

**Introduction.**

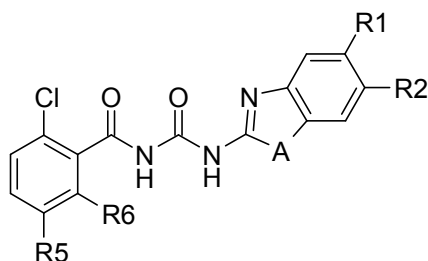
1  
2 Ghrelin, a 28 amino acid acylated peptide hormone is the endogenous ligand of the growth  
3 hormone secretagogue receptor type 1a (GHS-R1a).<sup>1</sup> The major physiological role of ghrelin appears to  
4 be in the control of food intake and energy homeostasis.<sup>2</sup> Energy intake and body weight are tightly  
5 regulated at a remarkably consistent set-point by control systems in the hypothalamus.<sup>3</sup> While the role  
6 of ghrelin in this system is still not fully understood, it is clear that acylated ghrelin is released from  
7 specialized mucosal cells in response to hunger cues. This results in a peak of plasma ghrelin levels  
8 before meal initiation<sup>4</sup> that is consistent with a role in meal initiation. In addition, ghrelin infusion in  
9 both rodents and humans increases appetite and food intake.<sup>5</sup> Consequently, peripheral and CNS  
10 penetrant ghrelin receptor antagonists have been proposed as potential therapeutic agents for the  
11 treatment of obesity<sup>6-11</sup> and type II diabetes.<sup>12</sup> Furthermore, due to the apparent high constitutive  
12 activity<sup>13-15</sup> of the ghrelin receptor demonstrated in recombinant cell systems and in rodents, inverse  
13 agonists may have additional benefit over 'neutral' antagonists in lowering the set-point for hunger  
14 between meals.<sup>16</sup>

15  
16 While several structurally diverse antagonists have been reported,<sup>17-30</sup> only a smaller number of  
17 these reports have identified inverse agonists.<sup>25-30</sup> Our aim was to identify GHS-R1a inverse agonists  
18 for the treatment of obesity and this manuscript details our efforts to obtain a new GHS-R1a chemotype  
19 which showed on-target efficacy in preclinical models.  
20  
21  
22  
23  
24  
25  
26  
27  
28  
29  
30  
31  
32  
33  
34  
35  
36  
37  
38  
39  
40  
41  
42  
43  
44  
45  
46  
47  
48  
49  
50  
51  
52  
53  
54  
55  
56  
57  
58  
59  
60

## Results and Discussion

High throughput screening (HTS) of the AstraZeneca compound collection was conducted and identified acylurea benzothiazole **1** as a suitable start point for optimization, having moderate binding affinity ( $IC_{50} = 0.21 \mu M$ ) for GHS-R1a but high lipophilicity and low aqueous solubility (Table 1). Removal of one chlorine as in compound **2** was tolerated for affinity, as was replacement of the methoxy group with methanesulfonyl which reduced lipophilicity (**3**). This resulted in an acceptable ligand lipophilicity efficiency (LLE),<sup>31</sup> which we aimed to maintain above 5 throughout optimisation. Further structural modifications were conducted to understand structure-activity relationships (SAR). Moving the sulfone group from the 6 to 5 position of the benzothiazole lost more than 10-fold affinity (**4**), while the corresponding benzoxazole **5** had no measurable affinity. To improve physicochemical properties, such as aqueous solubility, basic sidechains were appended to the 6-sulfonyl group in benzothiazoles **6-8**, resulting in retained affinity and solubilities exceeding  $50 \mu M$ . At the other end of the molecule, chemistry allowed us to explore SAR patterns around the phenyl ring. A notable 5-fold improvement in affinity was obtained by incorporation of a pyrrole group para to the Cl on the phenyl ring (**9**). Functional activity was then tested using a receptor-specific  $\beta$ -arrestin recruitment assay, Tango<sup>TM</sup>, in which the GHS-R1a was expressed from a T-REx<sup>TM</sup> inducible plasmid with high constitutive activity. This assay could differentiate agonists and inverse agonists,<sup>32</sup> and where measured, all compounds were shown to exhibit varying levels of partial agonism. Initially, this was not of concern as we wished to obtain high affinity first, and then explore SAR to convert functional activity to inverse agonism. This strategy was used successfully by us in a previously reported chemotype for the same receptor.<sup>28</sup>

**Table 1.** Initial SAR exploration optimisation.



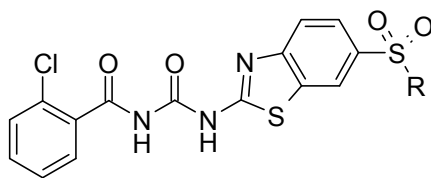
Cpd	R6	R5	A	R2	R1	h GHS-R1a binding $IC_{50}$ (nM) <sup>a,b</sup>	Agonist effect (%) <sup>a,c</sup>	LLE <sup>d</sup>	$\log D_{7.4}$	Aq. solubility ( $\mu M$ ) <sup>e</sup>
<b>1</b>	Cl	H	S	OMe	H	210	-	-	> 3.9	< 0.71
<b>2</b>	H	H	S	OMe	H	76	16	-	> 4	0.78
<b>3</b>	H	H	S	SO <sub>2</sub> Me	H	120	37	4.4	2.5	< 0.47
<b>4</b>	H	H	S	H	SO <sub>2</sub> Me	4700	10	2.5	2.8	3.0

1	5	H	H	O	SO <sub>2</sub> Me	H	> 10000	-	3.5	1.1	72
2	6	H	H	S	SO <sub>2</sub> (CH <sub>2</sub> ) <sub>2</sub> -pyrrolid-1-yl	H	44	65	4.7	2.7	64
3	7	H	H	S	SO <sub>2</sub> (CH <sub>2</sub> ) <sub>2</sub> -NH <sup>t</sup> Pr	H	27	82	5.2	2.3	71
4	8	H	H	S	SO <sub>2</sub> (CH <sub>2</sub> ) <sub>2</sub> -4-Me-piperazin-1-yl	H	83 <sup>f</sup>	51	5.6	1.5	240
5	9	H	pyrrol-1-yl	S	SO <sub>2</sub> Me	H	23	-	4.8	2.8	-

<sup>a</sup>Mean of at least 2 independent measurements, unless stated. <sup>b</sup>pIC<sub>50</sub> SEM <0.1 for cpds **1-5**, pIC<sub>50</sub> SEM <0.5 for cpds **6,7** and **9**. <sup>c</sup>Maximum % activation, maximum concentration = 10 μM. <sup>d</sup>Ligand lipophilicity efficiency, defined as GHS-R1a binding pIC<sub>50</sub> - logD<sub>7.4</sub>. <sup>e</sup>Aqueous solubility measured at pH 7.4, performed under thermodynamic conditions from solid samples. <sup>f</sup>n=1.

Further modification of the basic sulfonyl sidechain was conducted with the aim of increasing GHS-R1a affinity. A key SAR finding was that extension of the alkyl linker to three carbon atoms gave a step increase in potency (Table 2). An additional benefit of this homologation was to improve chemical stability by removing the potential for β-amino sulfones to eliminate the amino group. High LLE and good solubility was also achieved across the compound set with piperazine **14** exhibiting the highest affinity. With the potential for CNS exposure in mind, MDCK-MDR1 (Madin-Darby-canine-kidney cells transfected with MDR1, the human version of P-glycoprotein) permeability and efflux ratios were obtained.<sup>33</sup> High MDCK-MDR1 permeability ( $P_{app} > 5$ ) and low efflux (ratio < 5) were obtained except for diazepam **15**, which was a notable outlier exhibiting low permeability and high efflux. Again, all analogues were partial agonists, thus a couple of potent basic sidechains were selected for a more extensive assessment of SAR in combination with phenyl group modifications (Table 3).

**Table 2.** Optimising basic side chain for potency.



Cpd	R	h GHS-R1a binding IC <sub>50</sub> (nM) <sup>a,b</sup>	Agonist effect (%) <sup>a,c</sup>	LLE <sup>d</sup>	logD <sub>7.4</sub>	Aq. solubility (μM) <sup>e</sup>	MDCK-MDR1 P <sub>app</sub> A-B (x10 <sup>-6</sup> cm/s) / efflux ratio <sup>f</sup>
10	-(CH <sub>2</sub> ) <sub>3</sub> NMe <sub>2</sub>	8.7	71	6.4	1.7	240	13 / 1.4
11	-(CH <sub>2</sub> ) <sub>3</sub> NEt <sub>2</sub>	13	64	6.2	1.7	280	5.4 / 2.7
12		65	71	5	2.2	69	17 / 0.9
13	-(CH <sub>2</sub> ) <sub>3</sub> NH(CH <sub>2</sub> ) <sub>2</sub> OMe	8.6	51	6.8	1.3	87	-
14		1.3	77	7.1	1.8	280	7.1 / 4.2

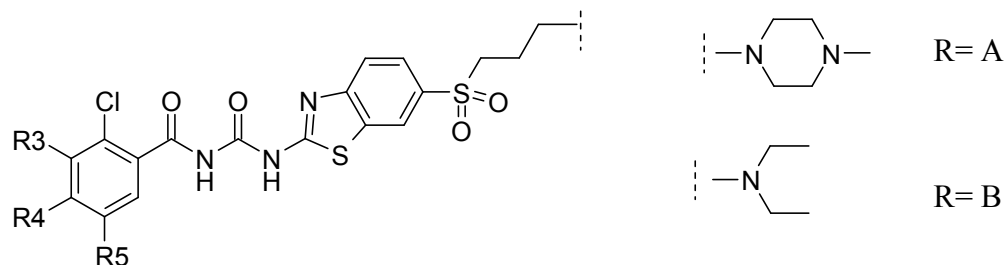


2  
3  
4  
5  
6  
7  
8  
9  
<sup>a</sup>Mean of at least 2 independent measurements. <sup>b</sup>pIC<sub>50</sub> SEM <0.27 for all examples. <sup>c</sup>Maximum % activation, maximum concentration = 10 μM. <sup>d</sup>Ligand lipophilicity efficiency, defined as GHS-R1a binding pIC<sub>50</sub> - logD<sub>7.4</sub>. <sup>e</sup>Aqueous solubility measured at pH 7.4, performed under thermodynamic conditions from solid samples. <sup>f</sup>Compounds were incubated at 10 μM in cultured MDCK-MDR1 cells and permeability was measured in both the A to B and B to A directions

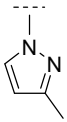
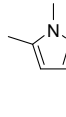
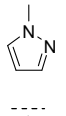
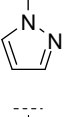
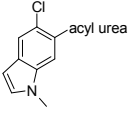
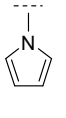
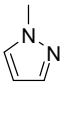
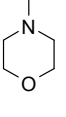
10                    The improvement in potency shown by the pyrrole group at R5 (**9**) indicated that this position  
11 was worth further exploration with different groups and additional aryl substituents. Small R5  
12 substituents (compounds **16-18**) maintained partial agonism and ethyl analogue **16** showed a 10-fold  
13 affinity increase concomitant with a lipophilicity increase that maintained LLE similar to the  
14 unsubstituted compound **14**. The larger ethoxy analogue **19** exhibited reduced partial agonism while  
15 still maintaining sub-nanomolar affinity. As expected, the combination of R5 pyrrole and a basic side  
16 chain yielded a good compound (**20**) which exhibited partial inverse agonism and sub-nanomolar  
17 affinity. Encouraged by this finding, we prepared other 5- and 6-membered rings, with pyrrolidine **21**,  
18 morpholine **22**, pyridine **23** and pyrazole **24** all showing high levels of inverse agonism and sub-  
19 nanomolar affinity. The SAR change from partial agonism to inverse agonism was specific and subtle.  
20 For example, moving the pyrazole to the R3 position (compound **25**), a large structural change, obliterated  
21 the inverse agonism with a 10-fold reduction in affinity. However, the small addition of a 3-methyl  
22 substituent to the pyrazole to give **26** also lost the inverse agonist activity but with maintained affinity.  
23 Moving the 3-methyl-pyrazole to the R4 position (compound **27**) resulted in a partial agonist with  
24 maintained affinity and further substitution to give the 3,5-di-methyl-pyrazole **28** resulted in high  
25 affinity and weak partial agonism. Consequently, to continue optimisation we focused on unsubstituted  
26 5/6-membered rings at R5 to assess the scope for maintaining inverse agonism with an additional group  
27 at R4. Gratifyingly, we were able to add diverse small substituents at R4 while maintaining high  
28 inverse agonism and sub-nanomolar affinity for compounds **29-31**. Combining R4 and R5 substituents  
29 through cyclisation in methyl-indole **32**, did not result in inverse agonism although sub-nanomolar  
30 affinity was maintained, which was consistent with a R5 substituent of appropriate size being the  
31 dominant determinant of inverse agonism. Three of the R5 groups giving highest inverse agonists were  
32 synthesized with a di-ethylamine at the opposite end of the molecule rather than a methyl-piperazine  
33 (compounds **33-35**). Affinity was reduced with di-ethylamine compared to methyl-piperazine as  
34 expected but surprisingly the pyrrole **33** no longer showed any inverse agonism while both pyrazole **34**  
35 and morpholine **35** maintained high inverse agonism. The subtle functional SAR we have uncovered for  
36 this chemical series appears to be heavily dependent on the R5 substituent but is also influenced by  
37 distal functional groups on the molecule. This makes predicting the functional activity of this series  
38 difficult and encouraged us to not settle on any one particular group but rather make a number of  
39  
40  
41  
42  
43  
44  
45  
46  
47  
48  
49  
50  
51  
52  
53  
54  
55  
56  
57  
58  
59  
60

combinations of groups at both ends of the molecule. In general, our findings are entirely consistent with reported mutagenesis studies where minor changes in peptide sequence had a major impact on biological activity at the ghrelin receptor.<sup>34</sup>

**Table 3.** Optimising for inverse agonism.



Cpd	R	R3	R4	R5	h GHS-R1a binding IC <sub>50</sub> (nM) <sup>a,b</sup>	Inverse agonist effect (%) <sup>a,c</sup>	Agonist effect (%) <sup>a,c</sup>	LLE <sup>d</sup>	logD <sub>7.4</sub>	MDCK-MDR1 P <sub>app</sub> A-B (x10 <sup>-6</sup> cm/s) / efflux ratio <sup>e</sup>	Rat po C <sub>max</sub> (μM) <sup>f</sup>	Rat B:P <sup>g</sup>	Rat free B:P <sup>h</sup>
16	A	H	H	Et	0.078	0	58	7.2	2.9	1.7 / 13	1.5	0.036	0.04
17	A	H	H	HC≡C	5.1	0	84	6	2.3	3.3 / 3.3	1.4	< 0.03	-
18	A	H	H	cPr	0.33	0	57	6.6	2.9	2.0 / 9.1	1.4	0.18	1.2
19	A	H	H	EtO	0.31	1	17	7.1	2.4	2.8 / 5.0	4.2	0.052	0.52
20	A	H	H		0.15	17	0	7.2	2.6	0.37 / 38	0.58	-	-
21	A	H	H		0.29	81	0	6.5	3.1	4.5 / 0.55	0.64	< 0.03	-
22	A	H	H		0.77	84	0	7.4	1.7	0.53 / 69	1.2	< 0.03	-
23	A	H	H		0.69	73	0	6.6	2.5	0.52 / 19	1	-	-
24	A	H	H		0.67	76	-	7.1	2	2.9 / 7.6	1.2	< 0.03	-
25	A		H	H	8.8	0	-	6.5	1.6	0.91 / 25	0.012	-	-
26	A	H	H		0.53	0	-	6.7	2.6	0.68 / 14	0.41	-	-

1	27	A	H		H	0.48	0	42	6.7	2.6	3.5 / 0.86	0.22	-	-
2														
3														
4														
5														
6	28	A	H	H		1.3	0	21	6.4	2.5	0.44 / 76	0.078	-	-
7														
8														
9														
10	29	A	H	MeO		0.62	76	0	7	2.2	0.86 / 46	-	-	-
11														
12														
13														
14	30	A	H	Cl		0.31	75	-	7.2	2.3	0.40 / 55	0.03	-	-
15														
16														
17														
18	31	A	H	N≡C		0.24	73	-	6.8	2.8	NV	-	-	-
19														
20														
21	32	A	H		acyl urea	0.57	0	-	6.4	2.8	3.9 / 0.71	0.3	0.049	0.04
22														
23														
24														
25														
26	33	B	H	H		0.43	0	-	6.4	2.9	0.10 / 42	3.6	-	-
27														
28														
29														
30	34	B	H	H		3.9	75	-	6.3	2.1	0.71 / 12	1.6	-	-
31														
32														
33														
34	35	B	H	H		2.9	75	-	6.7	1.8	3.3 / 5.5	9.4	< 0.01	-
35														

<sup>a</sup>Mean of at least 2 independent measurements. <sup>b</sup>pIC<sub>50</sub> SEM < 0.24 for all examples. <sup>c</sup>Maximum % activation, maximum concentration = 10 μM. <sup>d</sup>Ligand lipophilicity efficiency, defined as GHS-R1a binding pIC<sub>50</sub> - logD<sub>7.4</sub>. <sup>e</sup>Compounds were incubated at 10 μM in cultured MDCK-MDR1 cells and permeability was measured in both the A to B and B to A directions. <sup>f</sup>Compound was dosed PO at 2 mg/kg in 1% Pluronic F127. <sup>g</sup>Ratio of the drug concentrations in homogenized brain (B) tissue and plasma (P), 1 h after IV bolus then IV infusion. <sup>h</sup>Calculated using free fraction measured in plasma and brain (using either brain slice method<sup>35</sup> or brain homogenate)

For a number of compounds oral exposure in rat was assessed and modest to good levels were obtained for most compounds, including both agonists and inverse agonists (Table 3). Assessment of CNS exposure was conducted using rat infusion studies and it became apparent that generally very low levels were achieved in brain although compounds **18** and **19** did exhibit a free brain:plasma (B:P) ratios of 1.2 and 0.52 respectively. This generally low CNS exposure could be related to MDR1 mediated efflux in some cases and in all cases to low MDCK-MDR1 permeability ( $P_{app} < 5$ ). Notably morpholine **22** which was viewed as the lead inverse agonist at this time, had highest LLE and showed high oral exposure, but no detectable level in brain.

Evaluation of morpholine **22** against chemical properties generally associated with CNS medicinal agents revealed that efflux, polar surface area (PSA)<sup>36</sup> and rotatable bonds were parameters all outside the normal range.<sup>37</sup> Consequently, our strategy to improve brain exposure involved increasing MDCK-MDR1 permeability ( $P_{app} > 5$ ) and reducing MDCK-MDR1 efflux (ratio  $< 3$ ) through modification of the basic sidechain. We rationalized that reduced basicity could improve permeability and structural diversity may avoid efflux transporter recognition. The PSA of morpholine **22** was calculated as 124 Å but we reasoned that an intramolecular hydrogen bonding network involving the acylurea would exist. This effectively hides significant polarity making the actual PSA much less than calculated, and also effectively reduces hydrogen bond donor/acceptor and rotatable bond counts, so we were less concerned with reducing these three parameters. The flexible basic sidechain of **22** contributes to a high rotatable bond count of 12 and we targeted to reduce this. With these design considerations in mind, piperidinyl-sulfone **12** stood out from earlier compounds (Table 2) as containing the base most likely to afford CNS exposure going forward, with low efflux and lower rotatable bond count compared to other basic sidechains explored. Although affinity of this basic group was not as great as others, we rationalized that combination with optimal Cl-aryl substituents could yield a compound with overall balanced properties. Consequently, a small set of piperidinyl-sulfone compounds were prepared and profiled (Table 4). Substitution at R5 did improve affinity in all compounds and indeed this subset of compounds (**36-40**) displayed higher inverse agonism (80-96%) than previously seen, with the exception of methyl-indoline **41** which showed 69% inverse agonism. We had changed PK species from rat to mouse with a view to conducting efficacy studies in mouse and good oral exposure was obtained for this series. Some improvement in MDCK-MDR1 permeability and efflux was achieved, notably with morpholine **38**, which met our CNS design criteria. Gratifyingly, this did translate into significant brain exposure as measured in mouse (free B:P = 0.42). In general mouse brain data was consistent with rat infusion brain studies, for example compound **38** gave a free B:P = 1.3 in rat. A single crystal of **38** was obtained and X-ray crystallographic analysis<sup>38</sup> confirmed that the expected internally hydrogen bonded conformation did exist, where the hydrogen on the N connected to the benzothiazole interacts with the oxygen of the carbonyl connected to the aryl ring (Figure 1).

**Figure 1.** X-ray structure of **38**.

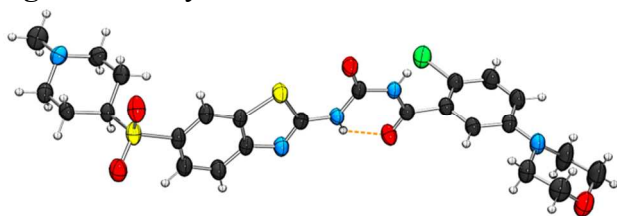
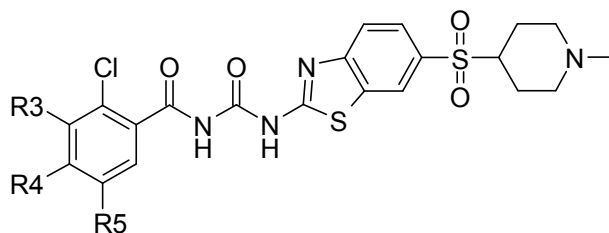


**Table 4.** Optimising for brain exposure.



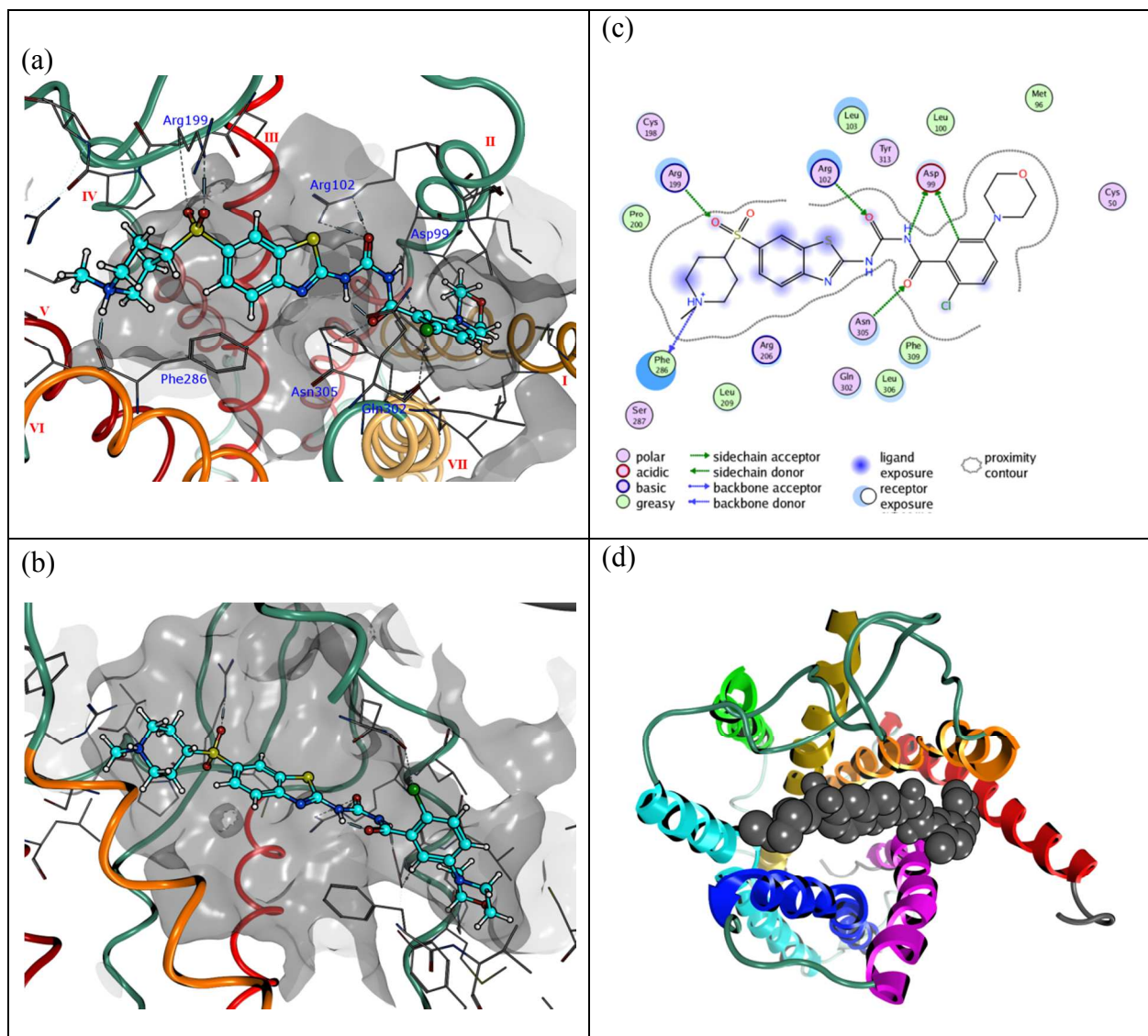
Cpd	R3	R4	R5	h GHS-R1a binding IC <sub>50</sub> (nM) <sup>a,b</sup>	Inverse agonist effect (%) <sup>a,c</sup>	LLE <sup>d</sup>	logD <sub>7.4</sub>	MDCK-MDR1 P <sub>app</sub> A-B (x10 <sup>-6</sup> cm/s) / efflux ratio <sup>e</sup>	Mouse po C <sub>max</sub> (μM) <sup>f</sup>	Mouse B:P (dose) <sup>g</sup>	Mouse free B:P <sup>h</sup>
36	H	H		15	96	5.3	2.5	3.9 / 2.5	1.5	-	-
37	H	H		33	81	4.9	2.6	1.1 / 15	0.64	0.90 (2 mg/kg)	0.61
38	H	H		6.7	92	5.9	2.3	5.4 / 2.6	6.5	0.21 (7 mg/kg)	0.42
39	H	H		0.92	88	5.9	3.1	11 / 0.05	5.8	-	-
40	H	N≡C		0.4	81	6.4	3	3 / 0.47	0.84	0.072 (0.9 mg/kg)	0.38
41	H			7.2	69	5.3	2.8	5.1 / 1.2	3	0.15 (2.7 mg/kg)	0.072

<sup>a</sup>Mean of at least 2 independent measurements. <sup>b</sup>pIC<sub>50</sub> SEM <0.20 for all examples. <sup>c</sup>Maximum % activation, maximum concentration = 10 μM. <sup>d</sup>Ligand lipophilicity efficiency, defined as GHS-R1a binding pIC<sub>50</sub> - logD<sub>7.4</sub>. <sup>e</sup>Compounds were incubated at 10 μM in cultured MDCK-MDR1 cells and permeability was measured in both the A to B and B to A directions. <sup>f</sup>Compound was dosed PO at 2 mg/kg in 1% Pluronic F127. <sup>g</sup>Ratio of the drug concentrations in homogenized brain (B) tissue and plasma (P), 6 h after PO dosing. <sup>h</sup>Calculated using free fraction measured in mouse plasma and rat brain (using either brain slice method<sup>35</sup> or brain homogenate).

In an attempt to understand the binding mode and subtle changes in SAR for functional activity, we created a homology model of GHS-R1a and docked our compounds into this model. The binding mode of these compounds is illustrated by compound **38** in Figure 2. The model predicts that the acylurea subunit makes several hydrogen-bonding interactions with Asp99, Arg102 (both TM2) and Asn305 (TM7). The sulfone group makes an interaction with Arg199 while the basic piperidine is pushed into a subpocket between TM4, TM5 and TM6. At the other end of the molecule, the bulk of the chlorine

atom causes the phenyl ring to twist out of the plane of the rest of the molecule, placing the morpholine group into a subpocket located between TM1, TM2 and TM7.

**Figure 2.** **38** bound into the ligand binding domain of the human GHS-R1a homology model. (a) 3D structure of the pocket, orientated down the transmembrane axis, viewed from the extracellular side, key residues and helices are labelled; (b) 3D structure of the pocket, orientated across the transmembrane axis; (c) 2D depiction of the binding mode and key interactions; (d) schematic image of the receptor showing the ligand braced between TM1 (red) and TM 5 (light-blue).



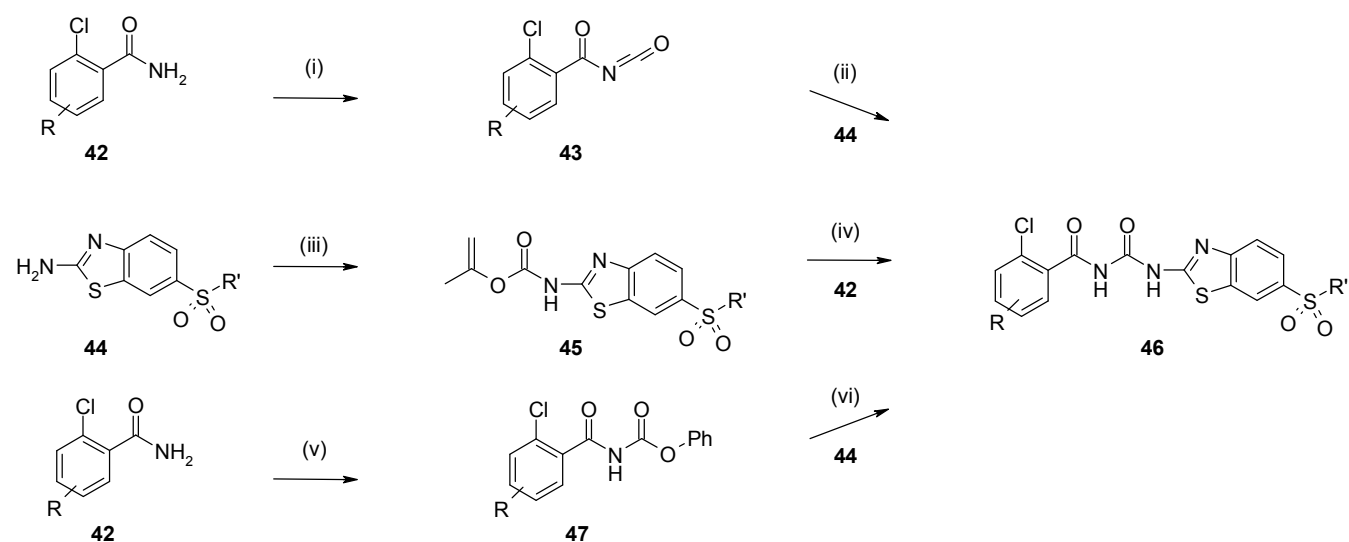
In terms of functional understanding of what favors agonism or inverse agonism, the proposed binding mode and mechanism of activation appears to be consistent with that proposed for the  $\beta_2$  adrenoceptor where TM5 moves towards the centre of the pocket upon activation.<sup>39</sup> In our model that region is occupied by the piperidine group, preventing this helix movement. In this context, the effect of the

morpholine group must also be invoked in order to fully explain inverse agonism SAR. It is inserted into a subpocket adjacent to TM1 which locks the binding mode, preventing lateral movement of the ligand that might allow TM5 to shift into the agonist conformation. Effectively, the molecule is a rigid unit, braced between TM1 and TM5. When the length of the brace is correct an inactive conformation of the receptor is induced and we observe inverse agonism. It is clear from the data presented that relatively bulky substituents at both ends of the molecule are required. However, inverse agonism is easily lost and subtle changes at either end of the molecule may result in sub-optimal interactions and allow partial or even full agonism. This is in agreement with our observed structure-function relationships in this series.

## Synthesis

Several synthesis routes were utilized in the preparation of acylureas (Scheme 1). In general, substituted benzamides **42** were reacted with oxalyl chloride in THF at 120 °C under microwave irradiation. Addition of the appropriate aminobenzothiazole **44** to the intermediate acyl isocyanate **43** and again heating to 120 °C gave the desired acylureas **46**. For more highly substituted substrates or those with acid sensitive functional groups present, an alternative method was employed. This involved synthesis of a carbamate intermediate such as **45** followed by microwave irradiation with the corresponding benzamide **44** under basic conditions. Alternatively benzoyl carbamates **47** were prepared, followed by reaction with the aminobenzothiazole **44** under neutral thermal conditions.<sup>40</sup>

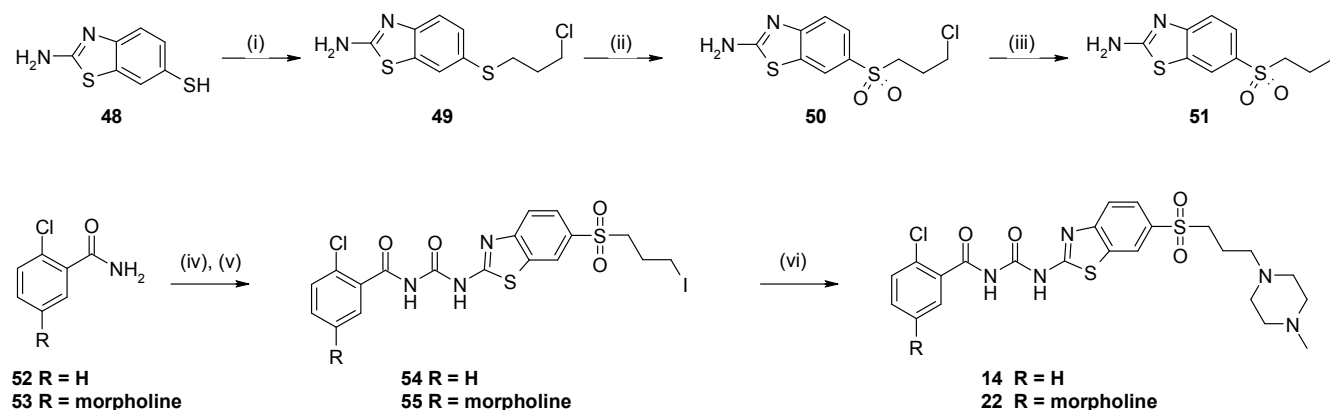
**Scheme 1.** General synthesis of acylureas<sup>a</sup>



<sup>a</sup>Reagents and conditions: (i) oxalyl chloride, THF, microwave, 120 °C, 1 h; (ii) DIPEA, rt, 1 h or microwave, 120 °C, 5 min; (iii) DIPEA, THF, isoprenylchloroformate, 0 °C; (iv) <sup>t</sup>BuOK, THF, reflux, 48 h; (v) NaH, (PhO)<sub>2</sub>C=O, THF, 1 h; (vi) 100 °C, 30 min.

To access the piperazine derivatives **14** and **22** we first needed to prepare the iodopropyl substituted aminobenzothiazole derivative **51** (Scheme 2). This was achieved in three steps from **48** which was converted to the thioether by reaction with 1-chloro-3-iodopropane. Subsequent oxidation to the sulfone with mCPBA and conversion to the iodide *via* a Finkelstein reaction gave **51**. The iodopropyl substituted acylurea **55** was prepared as above, and then without isolation this was converted to the methylpiperazine **22**. A similar procedure was followed for derivative **14** *via* isolation of intermediate **54**.

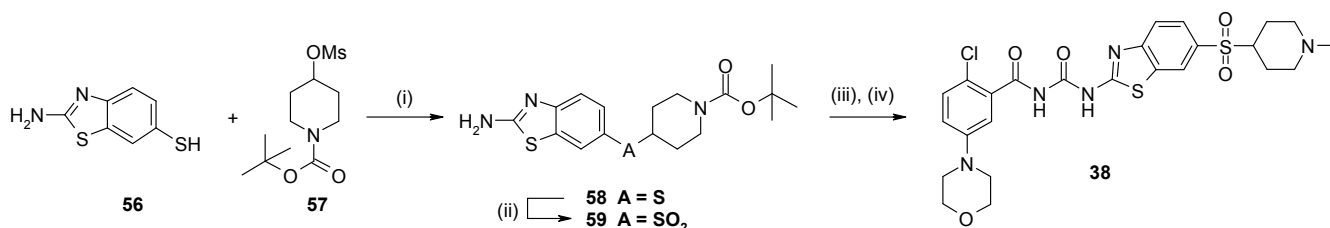
### Scheme 2. Synthesis of **14** and **22**<sup>a</sup>



<sup>a</sup>Reagents and conditions: (i)  $K_2CO_3$ , MeCN, 1-chloro-3-iodopropane; (ii) mCPBA, DCM, 38% (2 steps); (iii) NaI, acetone, reflux, 90%; (iv) oxalyl chloride (1 eq.); THF, microwave 120 °C, 5 min; (v) **51**, microwave 120 °C, 5 min, 35% (R=H, 2 steps); (vi) *N*-methylpiperazine, rt, 16 h, 58% (R=H), 16% (R=morpholine, 3 steps).

The methyl piperidine derivative **38** was accessed by first preparing the required aminobenzothiazole derivative **59** (Scheme 3). Reaction of the thiol **56** with mesylate **57** under reducing conditions to prevent formation of the disulfide gave the thioether **58**. This was oxidised to sulfone **59** and then converted to the acylurea as described previously which was subjected to Eschweiler-Clarke conditions that removed the protecting group and methylated the piperidine to give **38**.

### Scheme 3. Synthesis of **38**<sup>a</sup>



<sup>a</sup>Reagents and conditions: (i) K<sub>2</sub>CO<sub>3</sub>, NaBH<sub>4</sub>, MeCN/EtOH (9:1), 80 °C, 16 h, 92%; (ii) mCPBA, DCM, rt, 45 min, 68%; (iii) **53**, oxalyl chloride, THF, 120 °C, 15 min, then **59**, 120 °C; (iv) HCOOH, HCHO, 100 °C, 3 h, 15% (2 steps).

### Pharmacokinetic properties and Pharmacology of **14**, **22** and **38**.

Compounds **14**, **22** and **38**, which covered the range of in vitro function from partial agonism through to near full inverse agonism were profiled in vivo and demonstrated suitable PK properties in rat, mouse and dog (Table 5). Clearance was generally low, with **14** exhibiting the highest clearance of the three compounds, but relatively high plasma protein binding (PPB) free levels for **14** translated into low unbound clearance. Volume was consistent across the three species for each of the compounds and all showed sufficient oral exposure and bioavailability to be considered as useful in vivo tool compounds. Where measured, the affinity against rat and mouse isoforms of GHS-R1a was consistent with the data previously obtained for the human isoform (Table 5).

**Table 5.** Pharmacokinetic data for key in vivo compounds.

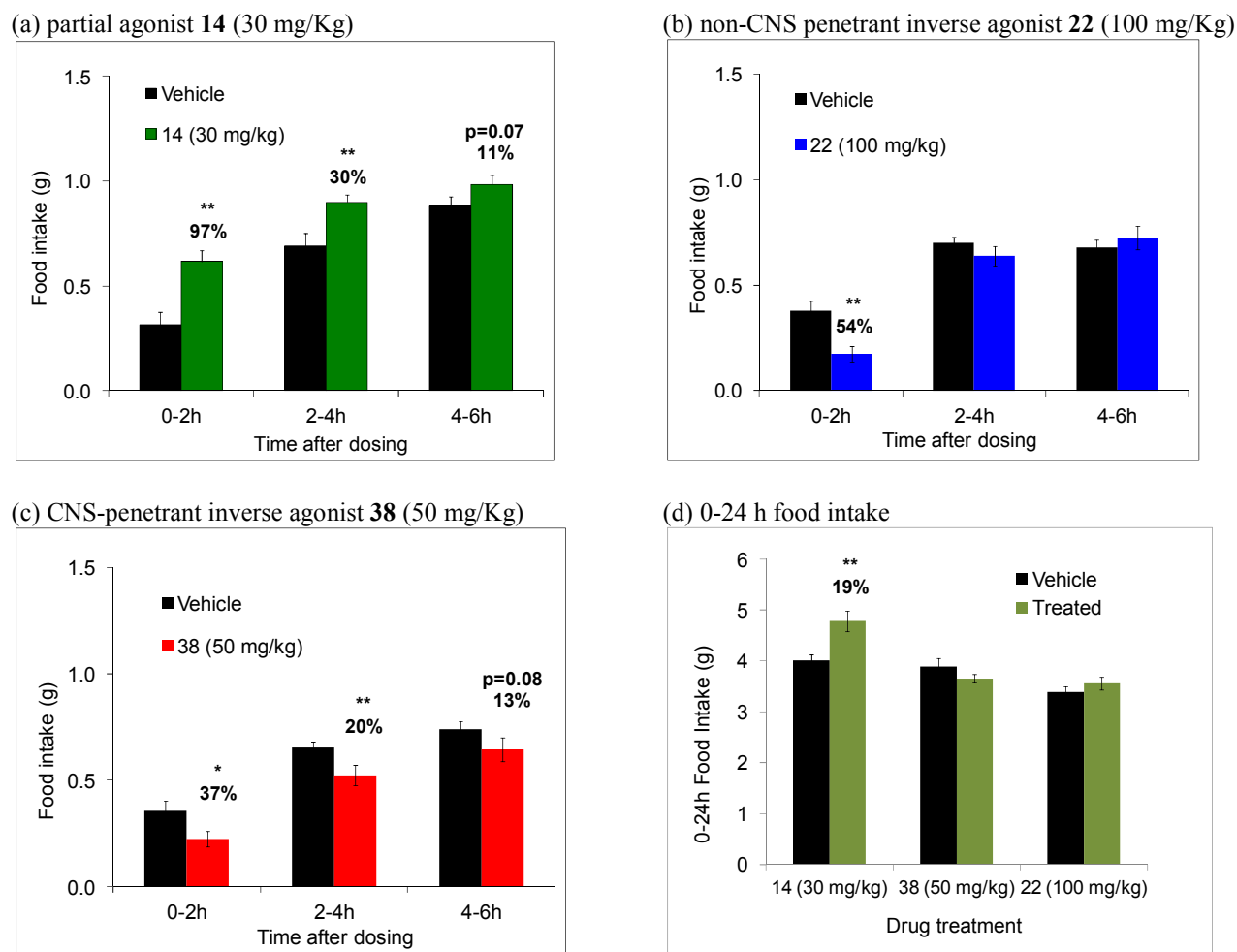
Cpd	Species	PPB % free	iv/po dose (mg/Kg) <sup>a</sup>	iv CL (mL/min/Kg)	iv V <sub>ss</sub> (L/Kg)	po C <sub>max</sub> (μM)	F (%)	GHS-R1a binding IC <sub>50</sub> (nM) <sup>b,c</sup>
<b>14</b>	Rat	8	2/2	24	4.9	0.34	125	3.6
	Mouse	13	2/5	35	4.5	0.71	40	4.9
	dog	9.6	1/1	8.1	4	0.2	51	-
<b>22</b>	Rat	0.35	2/2	2.6	0.9	0.58	30	3.4
	Mouse	0.6	2/1.3	2.9	0.8	1.3	50	1.1
	dog	0.78	2/2	0.69	0.3	11	87	-
<b>38</b>	Rat	0.2	2/2	1.9	0.7	4.5	171	-
	Mouse	0.9	2/7	1.8	0.4	8	25	39
	dog	1.6	2/2	10	0.4	1.0	31	-

<sup>a</sup>Compound was dosed IV in 5% DMSO:95% hydroxypropyl beta cyclodextrin; po in 1% Pluronic F127. <sup>b</sup>Mean of at least 2 independent measurements. <sup>c</sup>pIC<sub>50</sub> SEM <0.28 for all examples.

The three tool compounds were tested in mice to investigate the effects on normal food intake. Ad libitum fed mice were dosed to achieve maximum oral exposure at a time coinciding with peak food intake, at the beginning of the dark phase, and food intake measured in two-hourly intervals (Figure 3a-c). In this model, GHS-R1a agonist compounds including ghrelin and hexarelin induced a robust increase in food intake (data not shown) and this effect was replicated by the small-molecule partial agonist **14**. The effects of inverse agonists in this model appeared dependent on CNS penetration, as demonstrated by comparison of non-CNS penetrant inverse agonist **22** with CNS-penetrant inverse agonist **38**. At doses achieving significant free plasma cover over the receptor IC<sub>50</sub>, **22** achieved very

low CNS exposure, close to the levels from residual blood contamination of brain tissue, while **38** achieved free brain levels that gave free brain cover close to receptor IC<sub>50</sub> (Table 6). Compound **38** exhibited significant reduction in free feeding at each of the three 2 h time bins during the first 6 h of the study, while **22** exhibited a significant reduction in the earliest time bin but no effect during the 2-6 h time interval. There is a clear difference between the behavior of these two inverse agonists and the 0-2 h efficacy of **22** may be explained by a small amount of compound in the brain due to very high plasma exposure overcoming the high efflux observed for this compound. It is clear that free brain cover, rather than plasma cover, is driving the more significant 6 h effect shown by **38**. Neither inverse agonist has a significant effect in reducing food intake over a 24 h period, although partial agonist **14** did increase cumulative food intake over a 24 h period by 19% (Figure 3d).

**Figure 3.** Effect of compounds **14**, **22** and **38** on food intake in mouse free feeding model<sup>a</sup>



<sup>a</sup>Mean values  $\pm$  SEM (\* $p$ <0.05, \*\* $p$ <0.01, \*\*\* $p$ <0.001)

**Table 6.** PK multiples for compounds **14**, **22** and **38** in mouse free feeding model<sup>a</sup>

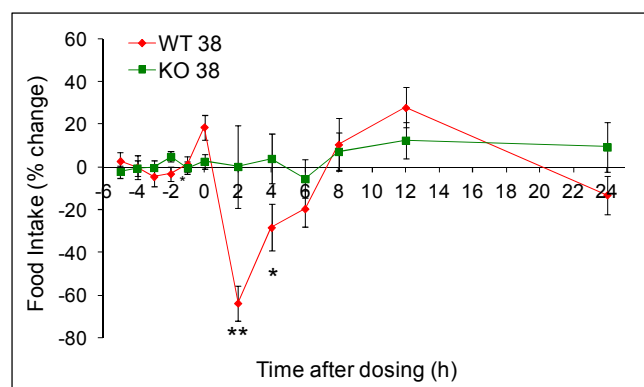
Cpd	po dose (mg/Kg)	free plasma multiple <sup>a</sup>			free brain multiple <sup>b</sup>		
		1 h	2 h	6 h	1 h	2 h	6 h

<b>14</b>	30	310	220	20	-	-	-
<b>22</b>	100	870	860	120	B:P < 0.01 <sup>c</sup>	B:P < 0.01 <sup>c</sup>	B:P < 0.01 <sup>c</sup>
<b>38</b>	50	14	13	3.5	0.40	-	0.43

<sup>a</sup>Oral exposure measured in plasma corrected for mouse PPB divided by mouse binding affinity. <sup>b</sup>Brain exposure corrected for rat brain %free divided by mouse binding affinity. <sup>c</sup>free B:P not determined because CNS exposure below a level that can be detected.

The specificity of the food-intake effect of **38** was investigated using genetically altered mice lacking the GHS-R1a receptor (Figure 4). In the wild-type (WT) mice, similar reductions in food intake over a 6 h period were observed compared to the previous experiments. In the null (KO) mice, no significant effects on food intake were observed, confirming that the effect of **38** is mediated via GHS-R1a. Furthermore, in vitro pharmacological profiling<sup>41</sup> of **38** against a panel of over 80 diverse targets was conducted and exhibited excellent selectivity (see supplementary information). Two targets showed activity below 1  $\mu$ M (dopamine transporter,  $K_i = 0.29 \mu$ M; nicotinic acetylcholine receptor  $\alpha 4$ ,  $K_i = 0.052 \mu$ M). A recent reported ghrelin inverse agonist was designed to avoid activity at the muscarinic receptor  $M_2$ .<sup>28</sup> Although **38** is an antagonist at  $M_2$ , it has 550-fold selectivity. In addition, **38** was inactive against hERG measured up to a maximum concentration of 33  $\mu$ M. Taking all this data together, **38** is clearly an excellent in vivo tool compound for exploring the inverse agonist pharmacology of the ghrelin receptor, and further studies will be reported in due course.

**Figure 4.** Effect of **38** (100 mg/Kg) on food intake in KO/WT mouse free feeding model<sup>a</sup>



<sup>a</sup>Mean values  $\pm$  SEM (\* $p < 0.05$ , \*\* $p < 0.01$ , \*\*\* $p < 0.001$ )

## Conclusion

Starting from HTS hit **1**, with moderate GHS-R1a affinity, we increased affinity and improved physicochemical properties by incorporation of a basic sulfone sidechain to afford partial agonist **14**. Further SAR optimization led to identification of inverse agonist **22** through discovery that adding a 5- or 6-membered ring at an appropriate position converted partial agonists into inverse agonists. Reduction of rotatable bond count and optimization of MDCK-MDR1 efflux led to increased brain

1 exposure in inverse agonist **38**. These three tool compounds showed good murine affinity for GHS-R1a  
2 and oral exposure and were dosed to free feeding mice. Partial agonist **14** caused increased acute food  
3 intake, while significant reduction of food intake over 6 h was observed with CNS penetrant inverse  
4 agonist **38** but not with non-CNS penetrant inverse agonist **22**. **38** also showed acute reduction of food  
5 intake in WT mice but not in KO mice. These results are consistent with free brain cover over GHS-  
6 R1a IC<sub>50</sub> being necessary for reduction of food intake, and that this effect occurs through a mechanism  
7 involving GHS-R1a.  
8  
9  
10  
11  
12  
13  
14  
15

## 16 Experimental Section

17  
18 **General.** All solvents and chemicals used were reagent grade. Anhydrous solvents THF,  
19 benzene, DCE, DCM and DME were purchased from Aldrich. Flash column chromatography was  
20 carried out using prepacked silica cartridges (from 4 g up to 330 g) from Redisep<sup>TM</sup> or Silicycle and  
21 eluted using an Isco Companion system. Purity and characterization of compounds were established by  
22 a combination of liquid chromatography-mass spectroscopy (LC-MS), gas chromatography-mass  
23 spectroscopy (GC-MS) and NMR analytical techniques and was >95% for all test compounds. <sup>1</sup>H NMR  
24 were recorded on a Varian INOVA (600 MHz), Varian Gemini 2000 (300 MHz) or Bruker Avance  
25 DPX400 (400 MHz) and were determined in CDCl<sub>3</sub> or DMSO-*d*<sub>6</sub>. Chemical shifts are reported in ppm  
26 relative to TMS (0.00 ppm) or solvent peaks as the internal reference. Splitting patterns are indicated as  
27 follows: s, singlet; d, doublet; t, triplet; m, multiplet; br, broad peak. Elevated temperatures were used  
28 where necessary to sharpen broad NMR peaks due to rotamers and the temperature used is noted for  
29 such compounds. Merck precoated TLC plates (silica gel 60 F<sub>254</sub>, 0.25 mm, art. 5715) were used for  
30 TLC analysis. Solutions were dried over anhydrous magnesium sulfate and the solvent was removed by  
31 rotary evaporation under reduced pressure.  
32  
33  
34  
35  
36  
37  
38  
39  
40  
41  
42  
43  
44

## 45 Synthesis of representative key examples (14, 22 and 38)

46 **6-(3-Chloropropylsulfanyl)benzothiazol-2-amine (49).** To a stirred solution of 2-  
47 aminobenzothiazole-6-thiol (10.0 g, 54.9 mmol) in MeCN (250 mL) was added potassium carbonate  
48 (11.4 g, 82.3 mmol) and 1-chloro-3-iodopropane (6.19 mL, 57.6 mmol) and the reaction mixture was  
49 heated at 85 °C for 1 h under nitrogen. The reaction mixture was cooled, filtered and the solid was  
50 washed with MeCN (2 x 100 mL), then the filtrate was concentrated *in vacuo* and the resulting solid  
51 was triturated with isohexane to give the title compound as a white solid (16.3 g) which was used  
52 without further purification. <sup>1</sup>H NMR (400 MHz, DMSO-*d*<sub>6</sub>) 1.89-1.97 (2H, m), 2.98 (2H, t), 3.72 (2H,  
53 t), 7.23-7.30 (2H, m), 7.55 (2H, s), 7.75 (1H, s); m/z MH<sup>+</sup> = 259.  
54  
55  
56  
57  
58  
59  
60

1  
2  
3  
4  
5  
6  
7  
8  
9  
10  
11  
12  
13  
14  
**6-(3-Chloropropylsulfonyl)benzothiazol-2-amine (50).** To a stirred solution of **49** (16.3 g, 89.9 mmol) in DCM (250 mL) was added mCPBA (32.6 g, 189 mmol) and the reaction mixture was stirred for 1 h, then washed with aqueous sodium metabisulfite (10% w/v, 100 mL) and saturated aqueous sodium bicarbonate solution (200 mL). The organic phase was dried (MgSO<sub>4</sub>), filtered, and concentrated *in vacuo* and then the resulting solid was triturated with isohexane to give the title compound as an orange solid (9.9 g, 38%) that was used without further purification. <sup>1</sup>H NMR (400 MHz, DMSO-d<sub>6</sub>) 1.95-2.02 (2H, m), 3.37-3.39 (2H, m), 3.68 (2H, t), 7.49 (1H, d), 7.67-7.70 (1H, m), 8.05 (2H, s), 8.25 (1H, d); m/z MH<sup>+</sup> = 291.

15  
16  
17  
18  
19  
20  
21  
22  
23  
24  
25  
26  
27  
28  
29  
**6-(3-Iodopropylsulfonyl)benzothiazol-2-amine (51).** To a stirred solution of **50** (6.0 g, 20.6 mmol) in acetone (100 mL) was added sodium iodide (30.9 mL, 206 mmol) and the reaction mixture was heated at 55 °C for 16 h. The reaction mixture was cooled, filtered and concentrated *in vacuo* and the residue was diluted with DCM (200 mL) and then washed with water (200 mL) and saturated brine (100 mL). The organic phase was dried, filtered and concentrated *in vacuo* and then the resulting solid was triturated with isohexane to give the title compound as an orange solid (7.1 g, 90%) that was used without further purification. <sup>1</sup>H NMR (400 MHz, DMSO-d<sub>6</sub>) 2.04 (2H, q), 3.27 (2H, t), 3.33 (2H, t), 7.48-7.51 (1H, m), 7.66-7.70 (1H, m), 8.06-8.07 (2H, s), 8.24 (1H, d); m/z MH<sup>+</sup> = 381.

30  
31  
32  
33  
34  
35  
36  
37  
38  
39  
40  
41  
42  
43  
44  
45  
46  
47  
48  
49  
50  
51  
**2-chloro-N-(6-(3-iodopropylsulfonyl)benzo[d]thiazol-2-ylcarbamoyl)benzamide (54).** Oxalyl chloride (2.71 mL, 31.6 mmol) was added to a stirred solution of 2-chlorobenzamide (**52**) (4.97 g, 31.9 mmol), in THF (270 mL) warmed to 60 °C, over a period of 5 min under nitrogen. The resulting solution was stirred at 60 °C for 90 min then evaporated. The residue in THF (20 mL) was added dropwise to a stirred solution of **51** (11.2 g, 29.4 mmol), and N-ethyl-N-isopropylpropan-2-amine (15.1 mL, 88.3 mmol) in THF (250 mL) over a period of 10 min under nitrogen. The resulting solution was stirred at rt overnight, diluted with EtOAc (250 mL), and washed sequentially with water (2 x 100 mL), and saturated brine (150 mL). The organic layer was dried (MgSO<sub>4</sub>), filtered, evaporated and purified by flash silica chromatography, elution gradient (0-40% EtOAc in DCM) to afford the title compound as a colorless solid (5.8 g, 35%). <sup>1</sup>H NMR (400 MHz, DMSO-d<sub>6</sub>) 2.10-2.26 (2H, m), 3.30-3.48 (2H, m), 3.48-3.52 (2H, m), 7.49-7.75 (4H, m), 7.98-8.16 (2H, m), 8.24 (1H, br), 11.70-12.10 (2H, br); m/z MH<sup>+</sup> = 563.

52  
53  
54  
55  
56  
57  
58  
59  
60  
**2-chloro-N-(((6-((3-(4-methylpiperazin-1-yl)propyl)sulfonyl)benzo[d]thiazol-2-yl)carbamoyl)benzamide (14).** 1-methylpiperazine (1.71 mL, 15.4 mmol) was added **54** (5.8 g, 10.3 mmol) in THF (40 mL). The resulting solution was stirred at rt overnight then heated to 50 °C for 5 h. The reaction mixture was diluted with EtOAc (150 mL), and washed sequentially with water (50 mL) and saturated brine (20 mL). The organic layer was dried (MgSO<sub>4</sub>), filtered and evaporated to afford

1 crude product. The crude product was purified by flash silica chromatography, elution gradient 0 to 20%  
2 MeOH in DCM. The crude product was triturated with Et<sub>2</sub>O to afford the title compound as a colorless  
3 solid (3.2 g, 58%). <sup>1</sup>H NMR (400 MHz, DMSO-d<sub>6</sub>) 1.69-1.73 (1H, m), 2.21 (4H, s), 2.30 (5H, q), 2.38  
4 (4H, s), 3.16 (2H, s), 3.33 (1H, s), 7.43-7.59 (4H, m), 7.83-7.88 (2H, m), 8.52 (1H, d); <sup>13</sup>C NMR (700  
5 MHz, DMSO-d<sub>6</sub>) δ 44.7, 51.4, 53.1, 54.0, 54.9, 119.9, 122.2, 125.1, 127.0, 128.8, 129.5, 129.6, 129.6,  
6 131.5, 132.4, 132.6, 135.3, 152.4, 152.7, 165.0, 168.4; HRMS (ES<sup>+</sup>) for C<sub>23</sub>H<sub>27</sub>ClN<sub>5</sub>O<sub>4</sub>S<sub>2</sub> (MH<sup>+</sup>): calcd  
7 536.1188; found, 536.1193.  
8  
9  
10  
11  
12

13 **2-Chloro-5-morpholin-4-yl-benzamide (53).** 2-Chloro-5-fluorobenzamide (1.0 g, 5.76 mmol)  
14 and morpholine (2.51 mL, 28.8 mmol) were dissolved in NMP (10 mL) and the reaction mixture was  
15 heated at 180 °C for 16 h then cooled, diluted with H<sub>2</sub>O (100 mL) and extracted with EtOAc (3 x 75  
16 mL). The combined organic phases were dried, filtered and concentrated to provide the crude product.  
17 Purification by flash silica chromatography elution gradient (0-100% EtOAc in isohexane) and  
18 trituration with Et<sub>2</sub>O afforded the title compound as a white solid (0.22 g, 15%): <sup>1</sup>H NMR (300 MHz,  
19 DMSO-d<sub>6</sub>) 3.11 (4H, t), 3.72 (4H, t), 6.93-6.99 (2H, m), 7.26 (1H, d), 7.47 (1H, s), 7.74 (1H, s); m/z  
20 MH<sup>+</sup> = 241.  
21  
22  
23  
24  
25  
26  
27

28 **N-(6-(3-(4-methylpiperazin-1-yl)propylsulfonyl)benzo[d]thiazol-2-ylcarbonyl)-5-**  
29 **morpholinobenzamide (22).** **53** (530 mg, 2.20 mmol) and oxalyl chloride (0.19 mL, 2.20 mmol) were  
30 suspended in THF (15 mL) and sealed into a microwave tube. The reaction was heated to 120 °C for 5  
31 min in the microwave reactor, then cooled to rt. The vial was cautiously degassed and opened. **51** (758  
32 mg, 1.98 mmol) was added portionwise and the suspension was stirred at 120 °C in the microwave for a  
33 further 5 min. The vial was cooled to rt and cautiously degassed. 1-methylpiperazine (0.733 mL, 6.61  
34 mmol) was added portionwise and the resulting suspension stirred at rt for 16 h. The reaction mixture  
35 was evaporated to dryness and the residue was purified by flash silica chromatography elution gradient  
36 (1-15% MeOH in DCM) to afford the title compound as a beige solid (220 mg, 16%). <sup>1</sup>H NMR (400  
37 MHz, DMSO-d<sub>6</sub>) 1.71-1.78 (2H, m), 2.38-2.47 (9H, m), 2.60 (4H, s), 3.18-3.20 (2H, m), 3.37 (4H, t),  
38 3.75 (4H, t), 7.11-7.14 (1H, m), 7.22 (1H, d), 7.40 (1H, d), 7.91-7.99 (2H, m), 8.65 (1H, d), 11.14 (2H,  
39 br s); <sup>13</sup>C NMR (700 MHz, DMSO-d<sub>6</sub>) δ 19.9, 44.6, 47.8, 51.3, 53.1, 54.0, 54.9, 65.8, 114.9, 117.8,  
40 118.8, 120.2, 122.4, 125.3, 130.0, 132.4, 132.9, 134.8, 149.4, 152.0, 152.3, 163.9, 168.4; HRMS (ES<sup>+</sup>)  
41 for C<sub>27</sub>H<sub>34</sub>ClN<sub>6</sub>O<sub>5</sub>S<sub>2</sub> (MH<sup>+</sup>): calcd 621.1715; found, 621.1719.  
42  
43  
44  
45  
46  
47  
48  
49  
50  
51  
52  
53

54 **tert-Butyl 4-(2-aminobenzothiazol-6-ylthio)piperidine-1-carboxylate (58).** To a solution of  
55 *tert*-butyl 4-(methylsulfonyloxy)piperidine-1-carboxylate<sup>42</sup> (**57**) (20.9 g, 74.8 mmol) in MeCN (900 mL)  
56 was added EtOH (100 mL), 2-aminobenzothiazole-6-thiol (**56**) (13.6 g, 74.8 mmol), potassium  
57 carbonate (13.4 g, 97.3 mmol) and sodium borohydride (8.50 g, 224 mmol). The suspension was heated  
58  
59  
60

1  
2  
3  
4  
5  
6  
7  
8  
9  
10  
11  
12  
13  
14  
15  
16  
17  
18  
19  
20  
21  
22  
23  
24  
25  
26  
27  
28  
29  
30  
31  
32  
33  
34  
35  
36  
37  
38  
39  
40  
41  
42  
43  
44  
45  
46  
47  
48  
49  
50  
51  
52  
53  
54  
55  
56  
57  
58  
59  
60

at 80 °C for 16 h under nitrogen. The reaction mixture was cooled, concentrated *in vacuo* and the residue was partitioned between H<sub>2</sub>O (900 mL) and DCM (900 mL). The aqueous phase was extracted with DCM (500 mL) and the combined organic phases were dried and concentrated to give the title compound as a yellow solid (25.1 g, 92%). <sup>1</sup>H NMR (400 MHz, DMSO-d<sub>6</sub>) 1.29-1.34 (2H, m), 1.38 (9H, s), 1.81-1.85 (2H, m), 2.85-2.87 (2H, m), 3.20 (1H, m), 3.81 (2H, m), 7.28 (2H, d), 7.54 (2H, s), 7.77 (1H, t); m/z (M-<sup>t</sup>Bu+H)<sup>+</sup> = 310.

**tert-Butyl 4-(2-aminobenzothiazol-6-ylsulfonyl)piperidine-1-carboxylate (59).** To a solution of **58** (31.8 g, 87.0 mmol) in DCM (900 mL) was added mCPBA (43.1 g, 183 mmol) portionwise. The solution was stirred for 45 min before addition of aqueous sodium metabisulphite (20% w/v, 500 mL). The organic phase was separated, washed with saturated aq. NaHCO<sub>3</sub> solution, dried (MgSO<sub>4</sub>) and filtered. A precipitate formed on standing, which was filtered to give the title compound (23.4 g, 39%). The filtrate was concentrated to 100 mL. Another precipitate formed on standing which was filtered to give a second crop of the title compound (9.9 g, 29%). <sup>1</sup>H NMR (400 MHz, DMSO-d<sub>6</sub>) 1.31-1.39 (11H, m), 1.83-1.86 (2H, m), 2.68-2.71 (2H, m), 3.38 (1H, t), 3.98-4.01 (2H, m), 7.49 (1H, d), 7.61-7.64 (1H, m), 8.01 (2H, s), 8.17 (1H, d); m/z (M-H)<sup>-</sup> = 396.

**2-Chloro-N-(6-(1-methylpiperidin-4-ylsulfonyl)benzothiazol-2-ylcarbamoyl)-5-morpholinobenzamide (38).** **53** (0.72 g, 3.0 mmol) and oxalyl chloride (0.28 mL, 3.15 mmol) were suspended in THF (15 mL) and heated at 120 °C in a microwave for 5 min. The reaction mixture was cooled and **59** (1.07 g, 2.70 mmol) was added. The reaction mixture was heated at 120 °C in a microwave for 5 min. The reaction mixture was cooled and concentrated. The residue was added to a mixture of acetyl chloride (10 mL) and MeOH (50 mL) (CAUTION, exotherm), stirred for 2 h and concentrated *in vacuo*. The residue was diluted with DCM (50 mL) and saturated aq. NaHCO<sub>3</sub> solution. The suspension was filtered to give crude 2-chloro-5-morpholino-N-(6-(piperidin-4-ylsulfonyl)benzothiazol-2-ylcarbamoyl)benzamide (1.02 g, 1.81 mmol). This was dissolved in formic acid (20 mL) and formaldehyde (37% w/w in H<sub>2</sub>O, 2.0 mL) added. The solution was heated at 100 °C for 3 h. The reaction mixture was concentrated *in vacuo* and the residue was dissolved in water. The solution was neutralized with saturated aq. NaHCO<sub>3</sub> solution and extracted with DCM (3 x 150 mL). The combined organic phases were concentrated *in vacuo* and purified by flash silica chromatography elution gradient (0-10% MeOH in DCM) to give the title compound as a white solid (0.23 g, 15%): <sup>1</sup>H NMR (400 MHz, DMSO-d<sub>6</sub>) 1.56-1.63 (2H, m), 1.83-1.97 (4H, m), 2.18 (3H, s), 2.88 (2H, d), 3.18 (4H, t), 3.75 (4H, t), 7.09-7.12 (1H, m), 7.20 (1H, d), 7.38 (1H, d), 7.83-7.86 (1H, m), 7.94 (1H, d), 8.57 (1H, d), 11.65 (2H, br s); <sup>13</sup>C NMR (176 MHz, DMSO-d<sub>6</sub>) 24.6, 45.0, 47.8, 53.2, 59.4, 65.8, 115.1, 118.0,

118.8, 120.4, 123.6, 126.3, 130.1, 130.8, 132.4, 134.4, 149.4, 151.3, 152.4, 162.9, 168.5;  $m/z$   $MH^+$  = 578; HRMS ( $ES^+$ ) for  $C_{25}H_{29}ClN_5O_5S_2$  ( $MH^+$ ): calcd, 578.1293; found, 578.1297.

### Homology modelling:

**Sequence alignment and structure building.** Three different GPCR structures were used as templates for the h GHS-R1a protein model. The closest available structure by sequence similarity is the rat Neurotensin Receptor Type 1, NTSR1 (pdb code = 4GRV<sup>43</sup>). This, alongside structures of the human Kappa Opioid Receptor, OPRK1 (pdb code = 4DJH<sup>44</sup>) and the human Substance-P Receptor, TACR1 (pdb code = 2KS9<sup>45</sup>) was aligned to the h GHS-R1a sequence automatically, using constraints based on principles previously described.<sup>46</sup> 4DJH was used as the template for TM helices 1 and 2; 2KS9 was used as the template for intracellular-loop 3; while 4GRV was used as template for the majority of the structure. Sequence alignment of these structures is included in the supplementary information. Choice of template was dictated by overall sequence similarity to h GHS-R1a and either Proline residue placement (in the case of helices) or loop length (in the case of loops). The sequence alignment and model construction was conducted in MOE (Chemical Computing Group) using the AMBER12 forcefield and default homology modelling parameters. The top model was accepted.

**Ligand placement.** MOE Site-Finder protocol was used to identify all enclosed pockets within the structure. The largest of these pockets was located within the transmembrane bundle, close to the extracellular side and bounded by the extracellular loops. These loops do not significantly descend into the pocket, leaving it relatively open. This pocket is most likely the binding site for the ghrelin hormone and was selected for docking studies. Docking was performed for the ligand molecules described herein using the MOE rigid-receptor docking protocol. Ligand conformations were constrained so that the acylurea unit forms a hydrogen-bonded pseudo-ring, as shown in the single-crystal X-ray structure of compound **38** (see Figure 2). The top-scoring ligand poses were manually inspected to select the most likely. Induced-fit docking (where pocket residues are mobile, but constrained) was subsequently performed on selected poses. Examination of the preferred binding modes for a range of ligands revealed a series of common interactions with the protein enabling selection of a single binding mode that was judged to be the best prediction of how these compounds bind to h GHS-R1a.

### Biological Protocols:

**<sup>125</sup>I-ghrelin displacement assay for GHS-R1a binding IC<sub>50</sub> determination (human, mouse or rat):** Isolated plasma membranes from HEK cells stably overexpressing the GHS-R1a receptor (4 $\mu$ g/well) were incubated for 60 min at rt with 20 pM [<sup>125</sup>I]human ghrelin (Perkin Elmer NEX388) in

1 the presence or absence of relevant concentrations of cold competing compounds. Incubations were  
2 performed in 100  $\mu$ L total volume of assay buffer (50 mM Tris-HCl, 5 mM MgCl<sub>2</sub>.6H<sub>2</sub>O, 0.01% BSA,  
3 pH7.4) containing 10  $\mu$ M methyl arachidonyl fluorophosphonate (Sigma M2939). The binding reaction  
4 was stopped by rapid filtration over Whatman GF/C filters pre-soaked with 0.5% polyethyleneimine and  
5 rinsed three times with ice-cold wash buffer (50 mM Tris-HCl, 5 mM MgCl<sub>2</sub>.6H<sub>2</sub>O, 50 mM NaCl,  
6 pH7.4) and the radioactivity bound to the membranes was measured using  $\gamma$ -counter.  
7  
8  
9  
10

11 **Invitrogen Tango functional assay:** Tango<sup>TM</sup> U2OS-GHS-R1a assay cells were plated at  
12 10,000 cells per well in 384-well plate in assay medium (100% Freestyle Medium containing 10 ng/mL  
13 doxycycline) in a final volume of 40  $\mu$ L and incubated overnight at 37 °C/5% CO<sub>2</sub>. Appropriate  
14 concentrations of compounds were also included at the time of plating. Following overnight incubation  
15 cells were loaded with LiveBLAzer FRET B/G substrate for 2 h at rt in the dark and the fluorescence  
16 emission values at 460 nm and 530 nm obtained using a FLIPR<sup>TETRA</sup> at 409 nm excitation. Maximal  
17 agonist response was measured relative to MK0677.  
18  
19  
20  
21  
22  
23  
24

25 **Mouse Free Feeding:** All animal experiments were conducted with strict adherence to licenses  
26 issued under the UK Animals (Scientific Procedures) Act 1986 and after local ethical review and  
27 approval. Studies described were performed under Home Office project license (PPL) number 40/3015.  
28 Male C57Bl6j, GHSr1<sup>-/-</sup>, and wildtype littermate controls were bred at AstraZeneca, Alderley Park.  
29 GHSr1<sup>-/-</sup> mice were generated by Deltagen (San Carlos, CA, USA) as previously described.<sup>47</sup> Male mice  
30 (6-8 weeks on arrival) were acclimatized for 3 weeks to a reversed light-dark cycle (9am-9pm DARK).  
31 Animals were group housed (3-5/cage) for 14 days then individually housed (1/cage) for 7 days.  
32 Baseline body weight & food intake were measured for the final 5 days before study. Animals were  
33 assigned to treatment groups (n=10-12) based on the average food intake and body weight recorded over  
34 4 days prior to study, so as to achieve similar means and variance in food intake and body weight in  
35 each group. Compounds were formulated the day before study as suspensions in 1% Pluronic F127  
36 (Sigma, St Louis, USA) in water. Compound or vehicle (10 mL/kg) was administered orally via gavage  
37 approximately 1 h prior to the onset of dark. After administration, animals were given access to a pre-  
38 weighed amount of food, which was subsequently re-weighed 2, 4, 6 and 24 h after administration.  
39  
40  
41  
42  
43  
44  
45  
46  
47  
48  
49  
50

51 **Pharmacokinetics:** Pharmacokinetic studies were performed in male Han-Wistar (HW) rats,  
52 beagle dogs and CD-1 mice. Intravenous (iv) administration was via bolus administration in a vehicle  
53 containing 5% DMSO 95% Hydroxy-propyl-B-Cyclodextrin 30% (W/V). Oral dosing was administered  
54 by gavage in a vehicle containing 0.1% F127 in water. Blood samples were collected over a 24 h period  
55 post dose into tubes containing EDTA-K2. Plasma was isolated by centrifugation, and the concentration  
56  
57  
58  
59  
60

1 of the test compound in plasma was determined by LC/MS/MS after protein precipitation with  
2 acetonitrile. Non-compartmental analysis was performed to estimate pharmacokinetic parameters using  
3 WinNonLin (version 5.0.1). All animal experiments were conducted with strict adherence to licenses  
4 issued under the UK Animals (Scientific Procedures) Act 1986 and after local ethical review and  
5 approval.  
6  
7  
8  
9  
10  
11  
12  
13  
14  
15  
16  
17  
18  
19  
20  
21  
22  
23  
24  
25  
26  
27  
28  
29  
30  
31  
32  
33  
34  
35  
36  
37  
38  
39  
40  
41  
42  
43  
44  
45  
46  
47  
48  
49  
50  
51  
52  
53  
54  
55  
56  
57  
58  
59  
60

1  
2 **Supporting Information.** Preparation and additional characterization for final compounds, enzymatic  
3 assay procedures, in vivo protocols for efficacy studies and homology model alignment. This material is  
4 available free of charge via the Internet at <http://pubs.acs.org>.  
5  
6  
7

### 8 9 **Corresponding Author**

10 Phone: +44(0)1625519444. E-mail: [william.mccoull@astrazeneca.com](mailto:william.mccoull@astrazeneca.com)  
11  
12

### 13 14 15 **Notes**

16 The authors declare no competing financial interest.  
17  
18  
19

### 20 21 **Acknowledgements**

22 Teresa Collins, Mark Denn and John Swales are acknowledged for expert technical assistance in  
23 generating DMPK data. Jenny Morrell, Elizabeth Strutynskyj, Steve Bloor, Rob Garcia, Sally Johnson,  
24 Susan Aiston and Julie Bartlett's expert technical assistance in generating affinity and functional data is  
25 also acknowledged. Duncan Armstrong, Philip Macfaul, Garry Pairaudeau and Matt Wood are thanked  
26 for useful discussions on this manuscript.  
27  
28  
29  
30  
31  
32

### 33 34 **Abbreviations Used**

35 DIPEA, diisopropylethylamine; FA, formic acid; GHS-R1a , growth hormone secretagogue receptor  
36 type 1a; h GHS-R1a, human isoform; m GHS-R1a, murine isoform; ; r GHS-R1a, rat isoform; LLE,  
37 ligand lipophilicity efficiency; MDCK, Madin-Darby canine kidney; MeCN, acetonitrile; TM, trans-  
38 membrane helix.  
39  
40  
41  
42

### 43 44 **References**

- 45  
46  
47 1. Kojima, M.; Hosoda, H.; Date, Y.; Nakazato, M.; Matsuo, H.; Kangawa, K. Ghrelin is a growth-  
48 hormone-releasing acylated peptide from stomach. *Nature (London)* **1999**, *402*, 656-660.  
49  
50  
51  
52  
53 2. Kojima, M.; Hosoda, H.; Matsuo, H.; Kangawa, K. Ghrelin: discovery of the natural endogenous  
54 ligand for the growth hormone secretagogue receptor. *Trends Endocrinol. Metab.* **2001**, *12*, 118-122.  
55  
56  
57  
58  
59  
60

- 1 3. Schwartz, M. W.; Woods, S. C.; Porte, D., Jr.; Seeley, R. J.; Baskin, D. G. Central nervous system  
2 control of food intake. *Nature (London)* **2000**, *404*, 661-671.
- 3  
4  
5  
6 4. Cummings, D. E.; Purnell, J. Q.; Frayo, R. S.; Schmidova, K.; Wisse, B. E.; Weigle, D. S. A  
7 preprandial rise in plasma ghrelin levels suggests a role in meal initiation in humans. *Diabetes* **2001**, *50*,  
8 1714-1719.
- 9  
10  
11  
12  
13  
14 5. Wren, A. M.; Seal, L. J.; Cohen, M. A.; Brynes, A. E.; Frost, G. S.; Murphy, K. G.; Dhillon, W. S.;  
15 Ghatei, M. A.; Bloom, S. R. Ghrelin enhances appetite and increases food intake in humans. *J. Clin.*  
16 *Endocrinol. Metab.* **2001**, *86*, 5992-5992.
- 17  
18  
19  
20  
21  
22  
23 6. Alvarez-Castro, P.; Pena, L.; Cordido, F. Ghrelin in obesity, physiological and pharmacological  
24 considerations. *Mini-Rev. Med. Chem.* **2013**, *13*, 541-552.
- 25  
26  
27  
28  
29 7. Depoortere, I. Targeting the ghrelin receptor to regulate food intake. *Regul. Pept.* **2009**, *156*, 13-23.
- 30  
31  
32  
33 8. Carpino, P. A.; Ho, G. Modulators of the ghrelin system as potential treatments for obesity and  
34 diabetes. *Expert Opin. Ther. Pat.* **2008**, *18*, 1253-1263.
- 35  
36  
37  
38 9. Soares, J.; Roncon-Albuquerque, R., Jr; Leite-Moreira, A. Ghrelin and ghrelin receptor inhibitors:  
39 agents in the treatment of obesity. *Expert Opin. Ther. Targets* **2008**, *12*, 1177-1189.
- 40  
41  
42  
43  
44 10. Zhao, H.; Liu, G. Growth hormone secretagogue receptor antagonists as anti-obesity therapies? Still  
45 an open question. *Curr. Opin. Drug Discovery Dev.* **2006**, *9*, 509-515.
- 46  
47  
48  
49  
50 11. Chollet, C.; Meyer, K.; Beck-Sickinger, A. G. Ghrelin-a novel generation of anti-obesity drug:  
51 design, pharmacomodulation and biological activity of ghrelin analogues. *J. Pept. Sci.* **2009**, *15*, 711-  
52 730.
- 53  
54  
55  
56  
57  
58  
59  
60

- 1  
2  
3  
4  
5  
6  
7  
8  
9  
10  
11  
12  
13  
14  
15  
16  
17  
18  
19  
20  
21  
22  
23  
24  
25  
26  
27  
28  
29  
30  
31  
32  
33  
34  
35  
36  
37  
38  
39  
40  
41  
42  
43  
44  
45  
46  
47  
48  
49  
50  
51  
52  
53  
54  
55  
56  
57  
58  
59  
60
12. Ahima, R. S. Antagonism of ghrelin for glycemic control in type 2 diabetes mellitus? *Endocrinology* **2007**, *148*, 5173-5174.
13. Damian, M.; Marie, J.; Leyris, J.; Fehrentz, J.; Verdie, P.; Martinez, J.; Baneres, J.; Mary, S. High constitutive activity is an intrinsic feature of ghrelin receptor protein: a study with a functional monomeric GHS-R1a receptor reconstituted in lipid discs. *J. Biol. Chem.* **2012**, *287*, 3630-3641.
14. Holst, B.; Cygankiewicz, A.; Jensen, T. H.; Ankersen, M.; Schwartz, T. W. High constitutive signaling of the ghrelin receptor-identification of a potent inverse agonist. *Mol. Endocrinol.* **2003**, *17*, 2201-2210.
15. Mokrosinski, J.; Frimurer, T. M.; Sivertsen, B.; Schwartz, T. W.; Holst, B. Modulation of constitutive activity and signaling bias of the ghrelin receptor by conformational constraint in the second extracellular loop. *J. Biol. Chem.* **2012**, *287*, 33488-33502.
16. Holst, B.; Schwartz, T. W. Constitutive ghrelin receptor activity as a signaling set-point in appetite regulation. *Trends Pharmacol. Sci.* **2004**, *25*, 113-117.
17. Rudolph, J.; Esler, W. P.; O'Connor, S.; Coish, P. D. G.; Wickens, P. L.; Brands, M.; Bierer, D. E.; Bloomquist, B. T.; Bondar, G.; Chen, L.; Chuang, C.; Claus, T. H.; Fathi, Z.; Fu, W.; Khire, U. R.; Kristie, J. A.; Liu, X.; Lowe, D. B.; McClure, A. C.; Michels, M.; Ortiz, A. A.; Ramsden, P. D.; Schoenleber, R. W.; Shelekhin, T. E.; Vakalopoulos, A.; Tang, W.; Wang, L.; Yi, L.; Gardell, S. J.; Livingston, J. N.; Sweet, L. J.; Bullock, W. H. Quinazolinone derivatives as orally available ghrelin receptor antagonists for the treatment of diabetes and obesity. *J. Med. Chem.* **2007**, *50*, 5202-5216.
18. Esler, W. P.; Rudolph, J.; Claus, T. H.; Tang, W.; Barucci, N.; Brown, S.; Bullock, W.; Daly, M.; DeCarr, L.; Li, Y.; Milardo, L.; Molstad, D.; Zhu, J.; Gardell, S. J.; Livingston, J. N.; Sweet, L. J. Small-molecule ghrelin receptor antagonists improve glucose tolerance, suppress appetite, and promote weight loss. *Endocrinology* **2007**, *148*, 5175-5185.

- 1  
2  
3  
4  
5  
6  
7  
8  
9  
10  
11  
12  
13  
14  
15  
16  
17  
18  
19  
20  
21  
22  
23  
24  
25  
26  
27  
28  
29  
30  
31  
32  
33  
34  
35  
36  
37  
38  
39  
40  
41  
42  
43  
44  
45  
46  
47  
48  
49  
50  
51  
52  
53  
54  
55  
56  
57  
58  
59  
60
19. Mihalic, J. T.; Kim, Y.; Lizarzaburu, M.; Chen, X.; Deignan, J.; Wanska, M.; Yu, M.; Fu, J.; Chen, X.; Zhang, A.; Connors, R.; Liang, L.; Lindstrom, M.; Ma, J.; Tang, L.; Dai, K.; Li, L. Discovery of a new class of ghrelin receptor antagonists. *Bioorg. Med. Chem. Lett.* **2012**, *22*, 2046-2051.
20. Puleo, L.; Marini, P.; Avallone, R.; Zanchet, M.; Bandiera, S.; Baroni, M.; Croci, T. Synthesis and pharmacological evaluation of indolinone derivatives as novel ghrelin receptor antagonists. *Bioorg. Med. Chem.* **2012**, *20*, 5623-5636.
21. Hanrahan, P.; Bell, J.; Bottomley, G.; Bradley, S.; Clarke, P.; Curtis, E.; Davis, S.; Dawson, G.; Horswill, J.; Keily, J.; Moore, G.; Rasamison, C.; Bloxham, J. Substituted azaquinazolinones as modulators of GHSr-1a for the treatment of type II diabetes and obesity. *Bioorg. Med. Chem. Lett.* **2012**, *22*, 2271-2278.
22. Sabbatini, F. M.; Melotto, S.; Bernasconi, G.; Bromidge, S. M.; D'Adamo, L.; Rinaldi, M.; Savoia, C.; Mundi, C.; Di Francesco, C.; Zonzini, L.; Costantini, V. J. A.; Perini, B.; Valerio, E.; Pozzan, A.; Perdonà, E.; Visentini, F.; Corsi, M.; Di Fabio, R. Azabicyclo[3.1.0]hexane-1-carbohydrazides as potent and selective GHSR1a ligands presenting a specific in vivo behavior. *ChemMedChem* **2011**, *6*, 1981-1985.
23. Serby, M. D.; Zhao, H.; Szczepankiewicz, B. G.; Kosogof, C.; Xin, Z.; Liu, B.; Liu, M.; Nelson, L. T. J.; Kaszubska, W.; Falls, H. D.; Schaefer, V.; Bush, E. N.; Shapiro, R.; Droz, B. A.; Knourek-Segel, V. E.; Fey, T. A.; Brune, M. E.; Beno, D. W. A.; Turner, T. M.; Collins, C. A.; Jacobson, P. B.; Sham, H. L.; Liu, G. 2,4-Diaminopyrimidine derivatives as potent growth hormone secretagogue receptor antagonists. *J. Med. Chem.* **2006**, *49*, 2568-2578.
24. Moulin, A.; Brunel, L.; Boeglin, D.; Demange, L.; Ryan, J.; M'Kadmi, C.; Denoyelle, S.; Martinez, J.; Fehrentz, J. The 1,2,4-triazole as a scaffold for the design of ghrelin receptor ligands: development of JMV 2959, a potent antagonist. *Amino Acids* **2013**, *44*, 301-314.

- 1  
2  
3  
4  
5  
6  
7  
8  
9  
10  
11  
12  
13  
14  
15  
16  
17  
18  
19  
20  
21  
22  
23  
24  
25  
26  
27  
28  
29  
30  
31  
32  
33  
34  
35  
36  
37  
38  
39  
40  
41  
42  
43  
44  
45  
46  
47  
48  
49  
50  
51  
52  
53  
54  
55  
56  
57  
58  
59  
60
25. Holst, B.; Lang, M.; Brandt, E.; Bach, A.; Howard, A.; Frimurer, T. M.; Beck-Sickinger, A.; Schwartz, T. W. Ghrelin receptor inverse agonists: identification of an active peptide core and its interaction epitopes on the receptor. *Mol. Pharmacol.* **2006**, *70*, 936-946.
26. Pasternak, A.; Goble, S. D.; de, J., Reynalda K.; Hreniuk, D. L.; Chung, C. C.; Tota, M. R.; Mazur, P.; Feighner, S. D.; Howard, A. D.; Mills, S. G.; Yang, L. Discovery and optimization of novel 4-[(aminocarbonyl)amino]-N-[4-(2-aminoethyl)phenyl]benzenesulfonamide ghrelin receptor antagonists. *Bioorg. Med. Chem. Lett.* **2009**, *19*, 6237-6240
27. Kung, D. W.; Coffey, S. B.; Jones, R. M.; Cabral, S.; Jiao, W.; Fichtner, M.; Carpino, P. A.; Rose, C. R.; Hank, R. F.; Lopaze, M. G.; Swartz, R.; Chen, H.; Hendsch, Z.; Posner, B.; Wielis, C. F.; Manning, B.; Dubins, J.; Stock, I. A.; Varma, S.; Campbell, M.; DeBartola, D.; Kosa-Maines, R.; Steyn, S. J.; McClure, K. F. Identification of spirocyclic piperidine-azetidine inverse agonists of the ghrelin receptor. *Bioorg. Med. Chem. Lett.* **2012**, *22*, 4281-4287.
28. McCoull, W.; Barton, P.; Broo, A.; Brown, A. J. H.; Clarke, D. S.; Coope, G.; Davies, R. D. M.; Dossetter, A. G.; Kelly, E. E.; Knerr, L.; MacFaul, P.; Holmes, J. L.; Martin, N.; Moore, J. E.; Morgan, D.; Newton, C.; Osterlund, K.; Robb, G. R.; Rosevere, E.; Selmi, N.; Stokes, S.; Svensson, T. S.; Ullah, V. B. K.; Williams, E. J. Identification of pyrazolo-pyrimidinones as GHS-R1a antagonists and inverse agonists for the treatment of obesity. *Med. Chem. Commun.* **2013**, *4*, 456-462.
29. McClure, K. F.; Jackson, M.; Cameron, K. O.; Kung, D. W.; Perry, D. A.; Orr, S. T. M.; Zhang, Y.; Kohrt, J.; Tu, M.; Gao, H.; Fernando, D.; Jones, R.; Erasga, N.; Wang, G.; Polivkova, J.; Jiao, W.; Swartz, R.; Ueno, H.; Bhattacharya, S. K.; Stock, I. A.; Varma, S.; Bagdasarian, V.; Perez, S.; Kelly-Sullivan, D.; Wang, R.; Kong, J.; Cornelius, P.; Michael, L.; Lee, E.; Janssen, A.; Steyn, S. J.; Lapham, K.; Goosen, T. Identification of potent, selective, CNS-targeted inverse agonists of the ghrelin receptor. *Bioorg. Med. Chem. Lett.* **2013**, *23*, 5410-5414.

- 1  
2  
3  
4  
5  
6  
7  
8  
9  
10  
11  
12  
13  
14  
15  
16  
17  
18  
19  
20  
21  
22  
23  
24  
25  
26  
27  
28  
29  
30  
31  
32  
33  
34  
35  
36  
37  
38  
39  
40  
41  
42  
43  
44  
45  
46  
47  
48  
49  
50  
51  
52  
53  
54  
55  
56  
57  
58  
59  
60
30. Bhattacharya, S. K.; Andrews, K.; Beveridge, R.; Cameron, K. O.; Chen, C.; Dunn, M.; Fernando, D.; Gao, H.; Hepworth, D.; Jackson, V. M.; Khot, V.; Kong, J.; Kosa, R. E.; Lapham, K.; Loria, P. M.; Londregan, A. T.; McClure, K. F.; Orr, S. T. M.; Patel, J.; Rose, C.; Saenz, J.; Stock, I. A.; Storer, G.; VanVolkenburg, M.; Vrieze, D.; Wang, G.; Xiao, J.; Zhang, Y. Discovery of PF-5190457, a potent, selective, and orally bioavailable ghrelin receptor inverse agonist clinical candidate. *ACS Med. Chem. Lett.* **2014**, *5*, 474-479.
31. Leeson, P. D.; Springthorpe, B. The influence of drug-like concepts on decision-making in medicinal chemistry. *Nat. Rev. Drug Discovery* **2007**, *6*, 881-890.
32. Hanson, B. J.; Wetter, J.; Bercher, M. R.; Kopp, L.; Fuerstenau-Sharp, M.; Vedvik, K. L.; Zielinski, T.; Doucette, C.; Whitney, P. J.; Revankar, C. A homogeneous fluorescent live-cell assay for measuring 7-transmembrane receptor activity and agonist functional selectivity through beta-arrestin recruitment. *J. Biomol. Screening* **2009**, *14*, 798-810.
33. Di, L.; Rong, H.; Feng, B. Demystifying brain penetration in central nervous system drug discovery. *J. Med. Chem.* **2013**, *56*, 2-12.
34. Els, S.; Schild, E.; Petersen, P. S.; Kilian, T.; Mokrosinski, J.; Frimurer, T. M.; Chollet, C.; Schwartz, T. W.; Holst, B.; Beck-Sickinger, A. G. An aromatic region to induce a switch between agonism and inverse agonism at the ghrelin receptor. *J. Med. Chem.* **2012**, *55*, 7437-7449.
35. Friden, M.; Ducrozet, F.; Middleton, B.; Antonsson, M.; Bredberg, U.; Hammarlund-Udenaes, M. Development of a high-throughput brain slice method for studying drug distribution in the central nervous system. *Drug Metab. Dispos.* **2009**, *37*, 1226-1233.
36. PSA was calculated using in-house software according to a published methodology: Ertl, P.; Rohde, B.; Selzer, P. Fast calculation of molecular Polar Surface Area as a sum of fragment-based contributions and its application to the prediction of drug transport properties. *J. Med. Chem.* **2000**, *43*, 3714-3717.

- 1  
2  
3  
4  
5  
6  
7  
8  
9  
10  
11  
12  
13  
14  
15  
16  
17  
18  
19  
20  
21  
22  
23  
24  
25  
26  
27  
28  
29  
30  
31  
32  
33  
34  
35  
36  
37  
38  
39  
40  
41  
42  
43  
44  
45  
46  
47  
48  
49  
50  
51  
52  
53  
54  
55  
56  
57  
58  
59  
60
37. Pajouhesh, H.; Lenz, G. Medicinal chemical properties of successful central nervous system drugs. *NeuroRX* **2005**, *2*, 541-553.
38. Crystal structure of **38**: Molecular formula = C<sub>25</sub>H<sub>28</sub>ClN<sub>5</sub>O<sub>5</sub>S<sub>2</sub>, C<sub>2</sub>H<sub>6</sub>O, 2(H<sub>2</sub>O), Formula weight = 578.11, 46.07, 36.04, Crystal system = Monoclinic, Space group = C 2/c,  $a = 30.3486(9) \text{ \AA}$ ,  $b = 16.2588(7) \text{ \AA}$ ,  $c = 14.5864(6) \text{ \AA}$ ,  $\alpha = 90^\circ$ ,  $\beta = 117.698(2)^\circ$ ,  $\gamma = 90^\circ$ ,  $V = 6372.6(4) \text{ \AA}^3$ ,  $T = 200\text{K}$ ,  $Z = 8$ ,  $D_c = 1.376(1) \text{ g cm}^{-3}$ ,  $\lambda_{(Mo-K\alpha)} = 0.71073$ ,  $\mu = 0.306 \text{ mm}^{-1}$ , 14180 reflections measured, 7257 independent reflections, 4077 observed reflections [ $I > 2.0 \sigma(I)$ ],  $R [F^2 > 2\sigma(F^2)] = 0.0806$ , Goodness of fit = 1.016. Crystallographic data have been deposited with the Cambridge Crystallographic Data Centre as supplementary publication number CCDC 997895.
39. Rasmussen, S. G. F.; Choi, H.; Fung, J. J.; Pardon, E.; Casarosa, P.; Chae, P. S.; DeVree, B. T.; Rosenbaum, D. M.; Thian, F. S.; Kobilka, T. S.; Schnapp, A.; Konetzki, I.; Sunahara, R. K.; Gellman, S. H.; Pautsch, A.; Steyaert, J.; Weis, W. I.; Kobilka, B. K. Structure of a nanobody-stabilized active state of the  $\beta_2$  adrenoceptor. *Nature (London, U. K.)* **2011**, *469*, 175-180.
40. Stokes, S.; Martin, N. G. A simple and efficient synthesis of N-benzoyl ureas. *Tetrahedron Lett.* **2012**, *53*, 4802-4804.
41. Bowes, J.; Brown, A. J.; Hamon, J.; Jarolimek, W.; Sridhar, A.; Waldron, G.; Whitebread, S. Reducing safety-related drug attrition: the use of in vitro pharmacological profiling. *Nat. Rev. Drug Discovery* **2012**, *11*, 909-922.
42. Northrup, A. B.; Katcher, M. H.; Altman, M. D.; Chenard, M.; Daniels, M. H.; Deshmukh, S. V.; Falcone, D.; Guerin, D. J.; Hatch, H.; Li, C.; Lu, W.; Lutterbach, B.; Allison, T. J.; Patel, S. B.; Reilly, J. F.; Reutershan, M.; Rickert, K. W.; Rosenstein, C.; Soisson, S. M.; Szewczak, A. A.; Walker, D.; Wilson, K.; Young, J. R.; Pan, B.; Dinsmore, C. J. Discovery of 1-[3-(1-Methyl-1H-pyrazol-4-yl)-5-oxo-5H-benzo[4,5]cyclohepta[1,2-b]pyridin-7-yl]-N-(pyridin-2-ylmethyl)methanesulfonamide (MK-

1 8033): A specific c-Met/Ron dual kinase inhibitor with preferential affinity for the activated state of c-  
2 Met. *J. Med. Chem.* **2013**, *56*, 2294-2310.  
3

4  
5  
6 43. White, J. F.; Noinaj, N.; Shibata, Y.; Love, J.; Kloss, B.; Xu, F.; Gvozdenovic-Jeremic, J.; Shah, P.;  
7 Shiloach, J.; Tate, C. G.; Grisshammer, R. Structure of the agonist-bound neurotensin receptor. *Nature*  
8 (*London, U. K.*) **2012**, *490*, 508-513.  
9

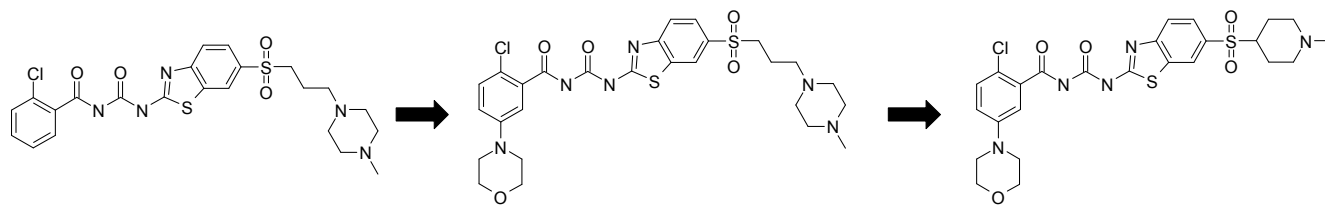
10  
11  
12  
13  
14 44. Wu, H.; Wacker, D.; Mileni, M.; Katritch, V.; Han, G. W.; Vardy, E.; Liu, W.; Thompson, A. A.;  
15 Huang, X.; Carroll, F. I.; Mascarella, S. W.; Westkaemper, R. B.; Mosier, P. D.; Roth, B. L.; Cherezov,  
16 V.; Stevens, R. C. Structure of the human  $\kappa$ -opioid receptor in complex with JD1c. *Nature (London, U.*  
17 *K.)* **2012**, *485*, 327-332.  
18  
19

20  
21  
22  
23  
24  
25 45. Gayen, A.; Goswami, S. K.; Mukhopadhyay, C. NMR evidence of GM1-induced conformational  
26 change of Substance P using isotropic bicelles. *Biochim. Biophys. Acta, Biomembr.* **2011**, *1808*, 127-  
27 139.  
28  
29

30  
31  
32  
33 46. Bissantz, C.; Logean, A.; Rognan, D. High-throughput modeling of human G-protein coupled  
34 receptors: Amino acid sequence alignment, three-dimensional model building, and receptor library  
35 screening. *J. Chem. Inf. Comput. Sci.* **2004**, *44*, 1162-1176.  
36  
37

38  
39  
40  
41 47. Egecioglu, E.; Jerlhag, E.; Salome, N.; Skibicka, K. P.; Haage, D.; Bohlooly-Y, M.; Andersson, D.;  
42 Bjursell, M.; Perrissoud, D.; Engel, J. A.; Dickson, S. L. Ghrelin increases intake of rewarding food in  
43 rodents. *Addict. Biol.* **2010**, *15*, 304-311.  
44  
45  
46  
47  
48  
49  
50  
51  
52  
53  
54  
55  
56  
57  
58  
59  
60

## Table of Contents Graphic



Compound	<b>14</b> (AZ-GHS-14)	<b>22</b> (AZ-GHS-22)	<b>38</b> (AZ-GHS-38)
GHS-R1a binding IC <sub>50</sub>	1.3 nM	0.77 nM	6.7 nM
GHS-R1a function	partial agonist	inverse agonist	inverse agonist
CNS exposure	-	non-CNS penetrant	CNS penetrant